The role of experiments and data reduction techniques in the tuning of different transition models

D. Simoni

Aerodynamics and Turbomachinery Laboratory
UNIVERSITY OF GENOVA

Contents

- ***Motivations*** *(what we are doing and why)*
- ***Experimental vs numerical data*** *(pro and cons)*
- ***Test case and BCs*** *(usability of the test case)*
- ***Example of possible learning procedures*** *(promoting sparsity)*
- ***Results and tuned models*** *(example of LKE, gamma-Re$_J$ and algebraic models)*

Motivations

- ***Hi-fidelity*** *simulations on* ***real applications*** *allow nowadays an* ***unprecedent view*** *of flow details*

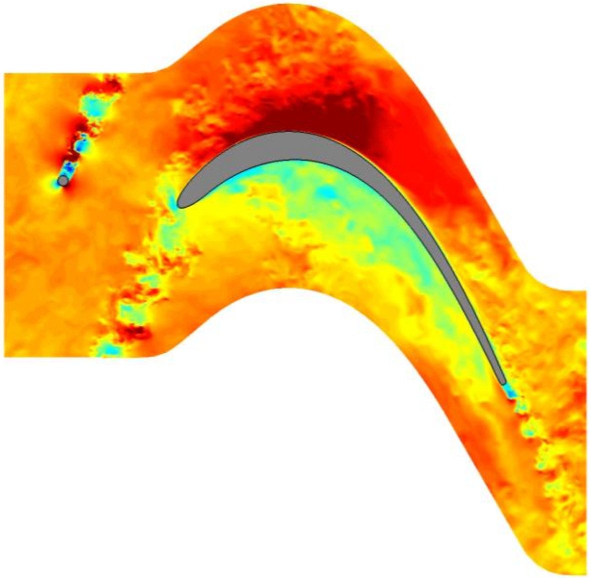

Motivations

- ***Hi-fidelity*** *simulations on* ***real applications*** *allow nowadays an* ***unprecedent view*** *of flow details*

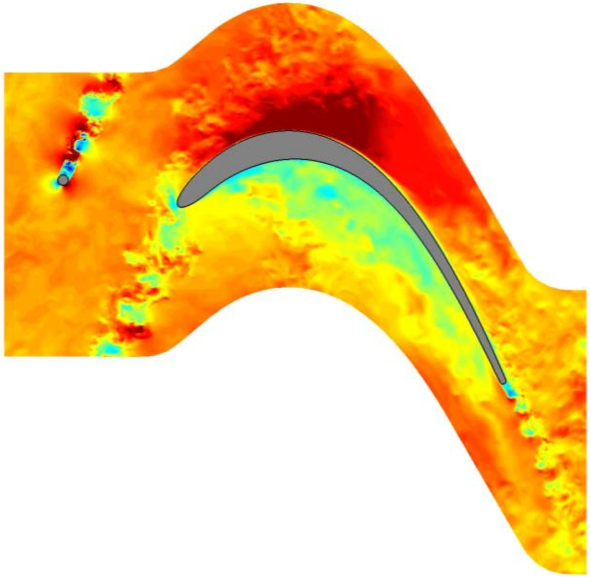

They are today still ***too costly*** *to be employed at* ***industrial level*** *to* ***sample*** *large region of* ***design space*** *variation*

Motivations

- ***Hi-fidelity*** *simulations on* ***real applications*** *allow nowadays an* ***unprecedent view*** *of flow details*

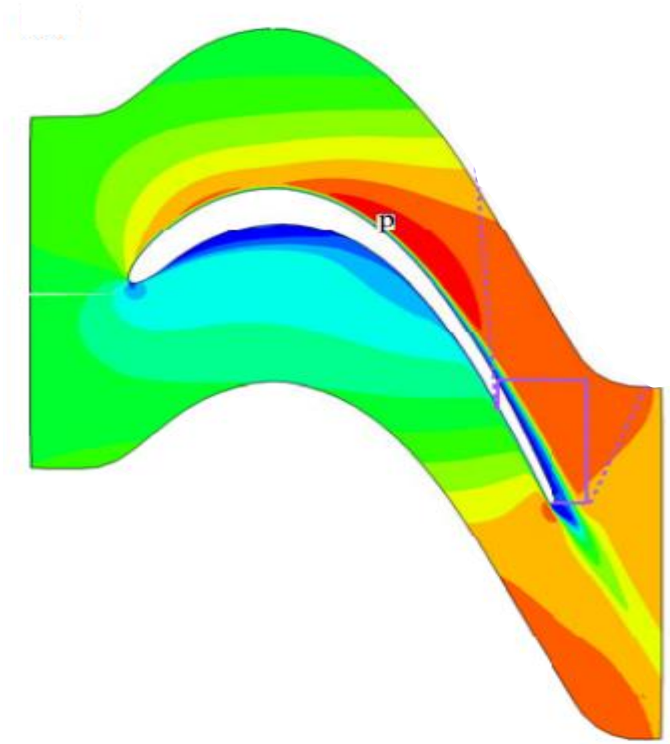

They are today still ***too costly*** *to be employed at* ***industrial level*** *to* ***sample*** *large region of* ***design space*** *variation*

RANS equations*, tuned with* ***hi-fidelity or high accuracy experimental*** *data, are the* ***best practice*** *actually used in industry to optimize aerodynamic components*

Motivations

- ***Hi-fidelity** simulations on **real applications** allow nowadays an **unprecedent view** of flow details*

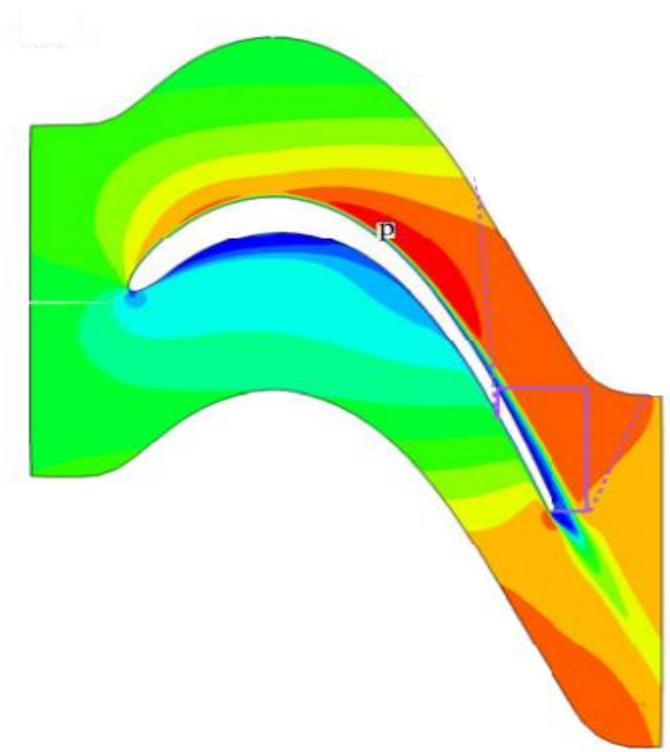

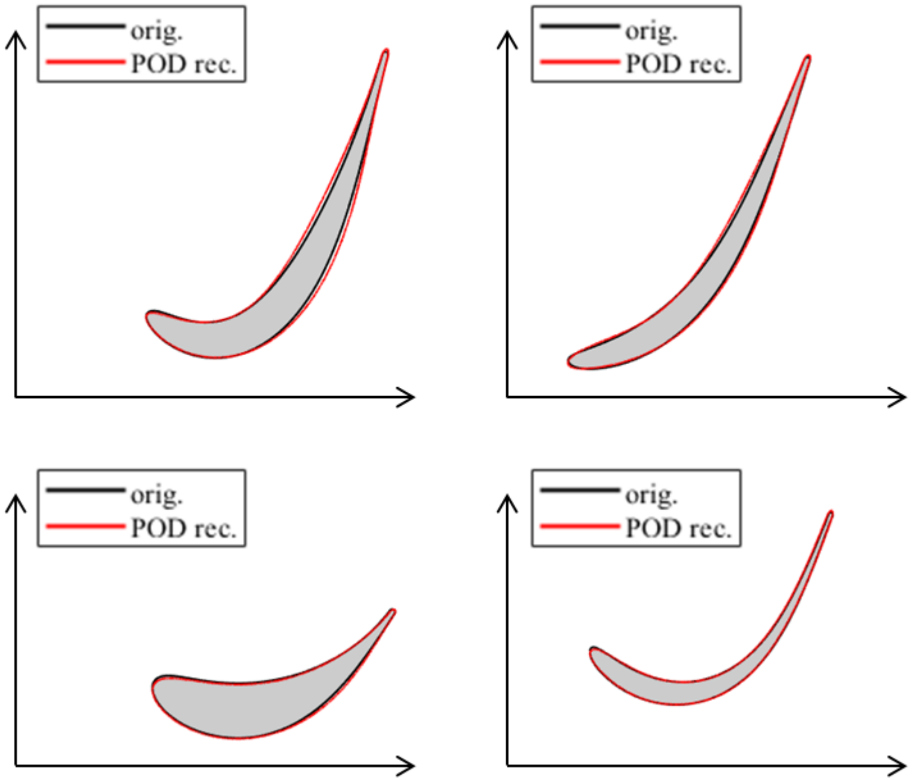

Motivations

- *The main target of the **RANS** approach is to **describe the effects of the turbulence** on the flow motion, without directly solving the Navier-Stokes equations, in order to **save computational time and cost**.*

- *This leads to obtain the **RANS** (Reynolds Average Navier-Stokes) equations:*

$$\frac{D\overline{\boldsymbol{U}}}{Dt} = -\frac{1}{\rho}\nabla\,\overline{p} + \nu\,\nabla^2\overline{\boldsymbol{U}} - \nabla\,([\boldsymbol{\tau}])$$

where: $\tau_{i,j} = \overline{u'_i u'_j}$

where: $\overline{\boldsymbol{U}}$ *is the average value describing the mean flow.*

$\boldsymbol{u}'$ *is the fluctuation describing the turbulent motion.*

- *The term* $([\boldsymbol{\tau}])$ *is known as the **Reynolds stress tensor** and requires **modelling strategies to close** the problem*

Motivations

*The most common and simplest tensor modeling strategies are **based on the Boussinesq's hypothesis,** that introduces an **eddy viscosity ν_t** providing a linear relationship between the stress and the strain tensor*

$$-\overline{u_i' u_j'} = \nu_t \left(\frac{\partial \overline{u_i}}{\partial x_j} + \frac{\partial \overline{u_j}}{\partial x_i} \right) + \left[-\frac{2}{3} \delta_{ij} k \right] \qquad \nu_t = f(k, \epsilon) = C_\mu \frac{k^2}{\epsilon} = C_\mu \sqrt{k} \frac{k^{3/2}}{\epsilon}$$

*This linear relation implies that principal axes of strain and modelled stress tensor will be aligned (which is unphysical, especially during transition), thus **non-linear models** account for of **tensor expansion of strain-rate and rotation**:*

$$-\overline{u_i' u_j'} = \nu_t S_{ij} + \nu_t' S_{ij} \Omega_{ij} + \nu_t'' S_{ij} S_{ij}^T + \nu_t''' S_{ij} \Omega_{ij} S_{ij}^T + \ldots$$

$$(\nu_t, \nu_t', \nu_t'' \ \ldots) = f(I_1, I_2, K, \varepsilon)$$

Pope, Stephen B. "A more general effective-viscosity hypothesis." *Journal of Fluid Mechanics* 72.2 (1975): 331-340.
Pope, Stephen B. *Turbulent flows*. Cambridge university press, 2000.

Motivations

The most common and simplest tensor modeling strategies are ***based on the Boussinesq's hypothesis,*** *that introduces an* ***eddy viscosity*** $\boldsymbol{\nu_t}$ *providing a linear relationship between the stress and the strain tensor*

$$-\overline{u_i'u_j'} = \nu_t \left(\frac{\partial \overline{u_i}}{\partial x_j} + \frac{\partial \overline{u_j}}{\partial x_i} \right) + \left[-\frac{2}{3}\delta_{ij}k \right] \qquad \nu_t = f(k,\epsilon) = C_\mu \frac{k^2}{\epsilon} = C_\mu \sqrt{k}\frac{k^{3/2}}{\epsilon}$$

This linear relation implies that principal axes of strain and modelled stress tensor will be aligned (which is unphysical, especially during transition), thus ***non-linear models*** *account for of* ***tensor expansion of strain-rate and rotation****:*

$$-\overline{u_i'u_j'} = \nu_t S_{ij} + \nu_t' S_{ij}\Omega_{ij} + \nu_t'' S_{ij}S_{ij}^T + \nu_t''' S_{ij}\Omega_{ij}S_{ij}^T + \ldots$$

$$(\nu_t, \nu_t', \nu_t'' \; \ldots.) = f(I_1, I_2, K, \varepsilon, features)$$

Pope, Stephen B. "A more general effective-viscosity hypothesis." *Journal of Fluid Mechanics* 72.2 (1975): 331-340.

Pope, Stephen B. *Turbulent flows*. Cambridge university press, 2000.

Motivations

- *Irrespective of the constitutive law for the modelling of the stress tensor (i.e. linear or not linear)* ***two additional differential equations****, one for the* ***turbulent kinetic energy*** *and the other for the* ***dissipation term*** *ε are fundamental ingredient of common RANS solvers:*

$$\begin{cases} \dfrac{D\overline{\boldsymbol{U}}}{Dt} = -\dfrac{1}{\rho}\boldsymbol{\nabla}\left(\overline{p} + \dfrac{2}{3}K\right) + (\nu + \nu_T)\boldsymbol{\nabla}^2\overline{\boldsymbol{U}} \\ \dfrac{DK}{Dt} = P_K + D_K - \varepsilon \\ \dfrac{D\varepsilon}{Dt} = P_\varepsilon + D_\varepsilon - \varepsilon_\varepsilon \end{cases}$$

P indicates ***energy production****, D* ***diffusion*** *and ε* ***dissipation*** *of the related quantity*

Motivations

- *Irrespective of the constitutive law for the modelling of the stress tensor (i.e. linear or not linear)* ***two additional differential equations****, one for the* ***turbulent kinetic energy*** *and the other for the* ***dissipation term*** *ε are fundamental ingredient of common RANS solvers:*

$$\begin{cases} \dfrac{D\overline{\boldsymbol{U}}}{Dt} = -\dfrac{1}{\rho}\boldsymbol{\nabla}\left(\overline{p} + \dfrac{2}{3}K\right) + (\nu + \nu_T)\boldsymbol{\nabla}^2\overline{\boldsymbol{U}} \\ \dfrac{DK}{Dt} = \gamma P_K + D_K - \varepsilon \\ \dfrac{D\varepsilon}{Dt} = P_\varepsilon + D_\varepsilon - \varepsilon_\varepsilon \end{cases}$$

P indicates ***energy production****, D* ***diffusion*** *and ε* ***dissipation*** *of the related quantity*

Additionally, ***the eddy viscosity (or the production of K)*** *should be* ***"activated/deactivated"*** *by means of ad hoc tuned* ***intermittency function (γ),*** *acting like a* ***"transition model"*** *avoiding the excessive diffusion of the turbulence*

Generally, also the ***intermittency function*** *is described by algebraic or partial differential equations requiring in both cases fine tuning of relative ingredients*

Motivations

- ***Other*** ***transition models*** *have been developed with its own coefficients and blending functions to be tuned*

Motivations

- ***Other*** ***transition models*** *have been developed with its own coefficients and blending functions to be tuned*

Generally, the terms of the equations ***need to be tuned*** *by means of* **big data sets***,*

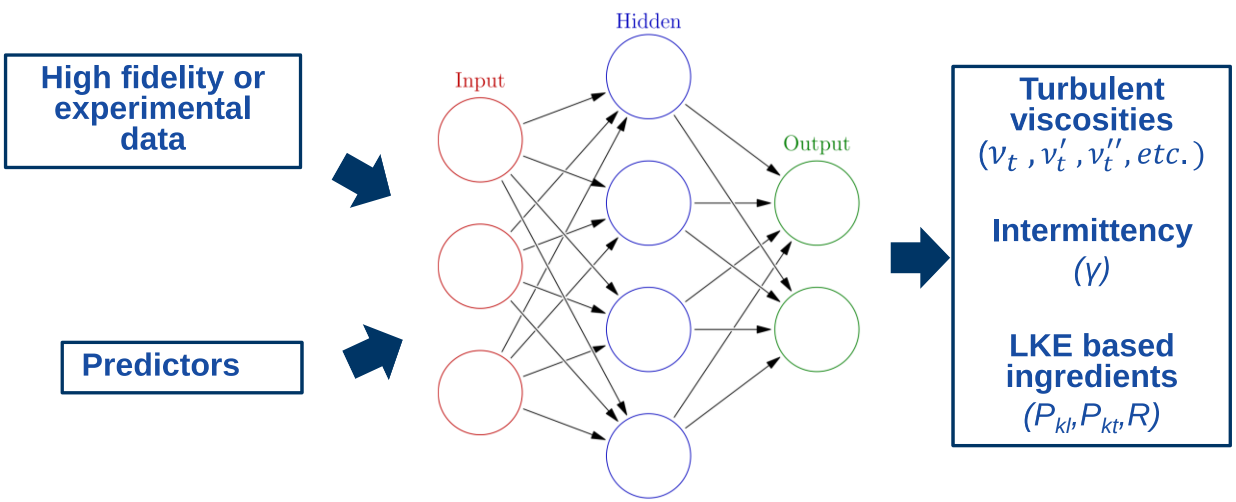

Motivations

- ***Other*** ***transition models*** *have been developed with its own coefficients and blending functions to be tuned*

Generally, the terms of the equations ***need to be tuned*** *by means of* ***big data sets****, involving the main* ***flow features*** *affecting the transition, like for example the* ***Reynolds number*** *(Re), the free-stream* ***turbulence level*** *(Tu) and additional ones (i.e.* ***vorticity, turbulent Re number, strain and rotation tensor invariants…..****).*

feature	definition
I_1	$S^*_{mn}S^*_{mn}$
I_2	$\Omega^*_{mn}\Omega^*_{mn}$
Re_k	$\frac{\sqrt{k}y}{\nu} * 10^{-2}$
Re_Ω	$\frac{\sqrt{I_2}y^2}{\nu} * 10^{-1}$
Π_2	$\frac{\lVert\Omega\rVert y}{\lVert U\rVert} * 10^{-1}$
Π_5	$\frac{k}{\nu\lVert\Omega\rVert} * 10^{-2}$
Π_6	$\frac{\lVert S\rVert y}{\lVert U\rVert} * 10^{-2}$
Π_k	$\frac{\lVert S\rVert y}{\sqrt{k}} * 10^{-1}$
η_1	$\frac{\lVert\Omega\rVert^2 - \lVert S\rVert^2}{\lVert\Omega\rVert^2 + \lVert S\rVert^2}$
η_2	$\frac{k}{0.5U_iU_i + k}$

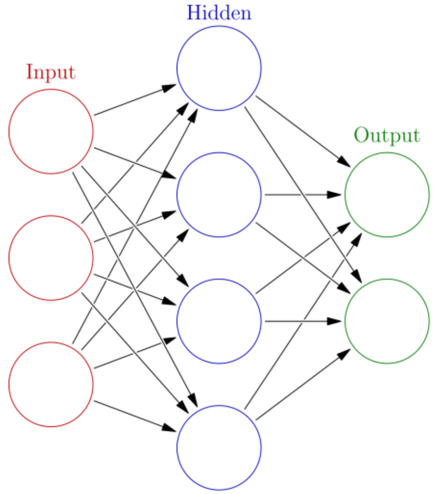

Turbulent viscosities
$(\nu_t, \nu_t', \nu_t'', etc.)$

Intermittency
(γ)

LKE based ingredients
(P_{kl}, P_{kt}, R)

Experimental vs numerical data

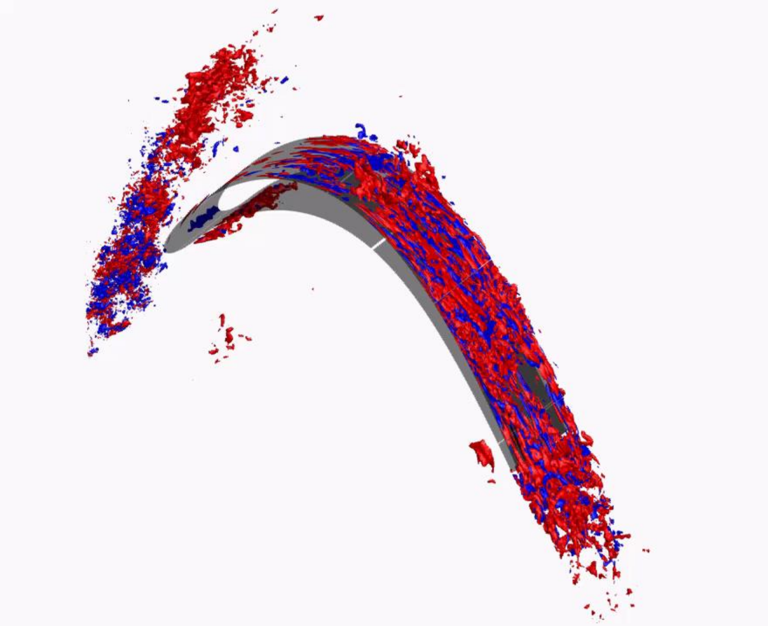

Hi-fi data allows:

- *high spatial and temporal resolutions*
- *detail of the full domain and 3D results*

They exibit limited:

- number of snapshot stored

- conditions tested due to numerical cost

Experimental vs numerical data

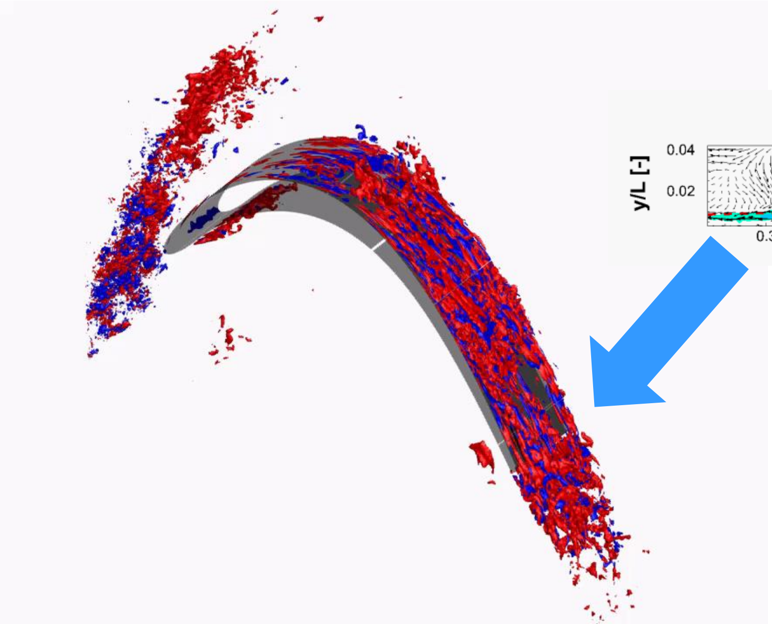

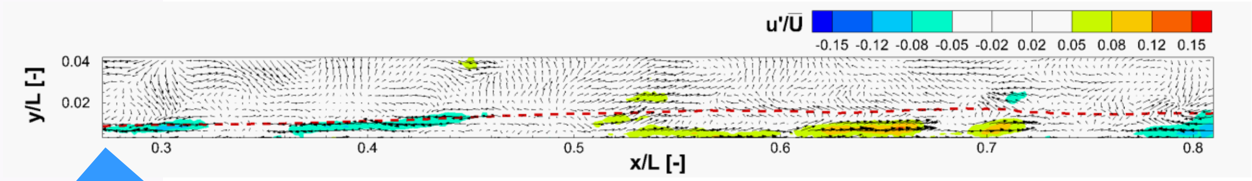

Hi-fi data allows:

- *high spatial and temporal resolutions*
- *detail of the full domain and 3D results*

They exibit limited:

- number of snapshot stored

- conditions tested due to numerical cost

Experiments data allows:

- *Quick variation of flow condistions*
- *Large number of stored shapshots*

They exibit limited:

- Spatial resolution

- Limited portion of the domain investigated

Experimental vs numerical data

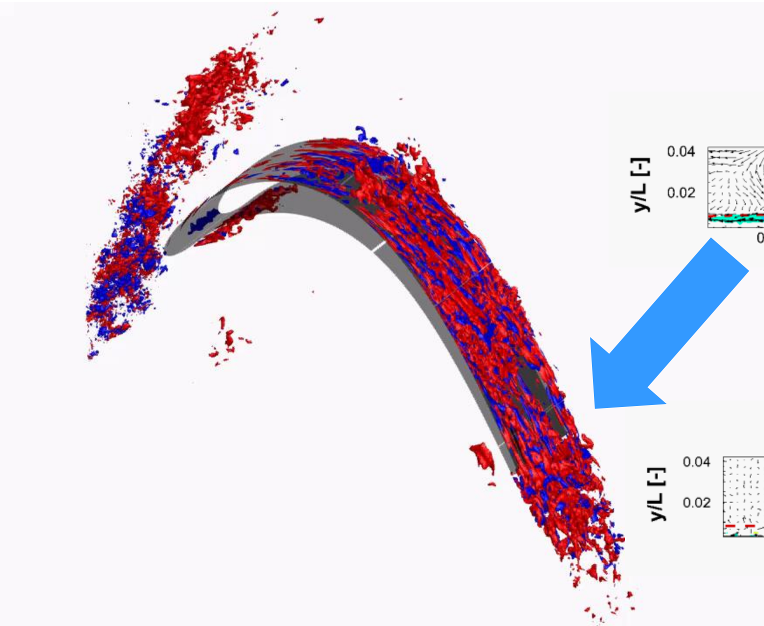

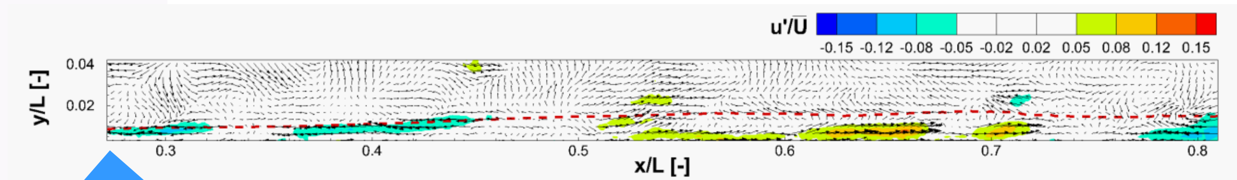

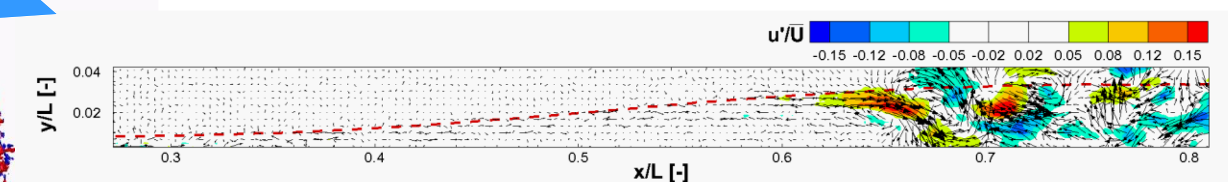

Hi-fi data allows:

- *high spatial and temporal resolutions*
- *detail of the full domain and 3D results*

They exibit limited:

- number of snapshot stored

- conditions tested due to numerical cost

Experiments data allows:

- *Quick variation of flow condistions*
- *Large number of stored shapshots*

They exibit limited:

- Spatial resolution and generally 2D analysis

- Limited portion of the domain investigated

Test case and BCs

FLAT PLATE
- *Elliptic L.E. (4:1)*
- *L = 300 mm*
- *W = 300 mm*

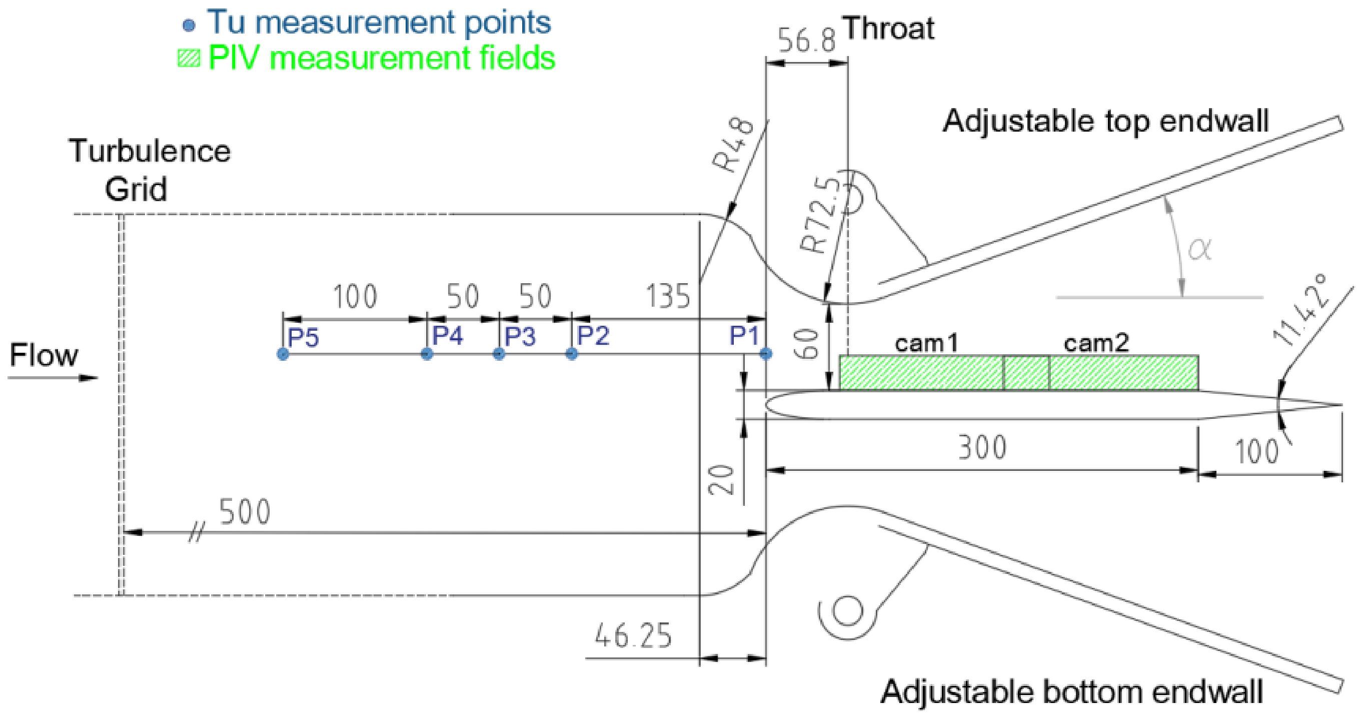

HW measurements to characterize the incoming flow

PIC measurements with a doble camera (cam1, cam2) layout to obtain high spatial resolution and large field of view

Test case and BCs

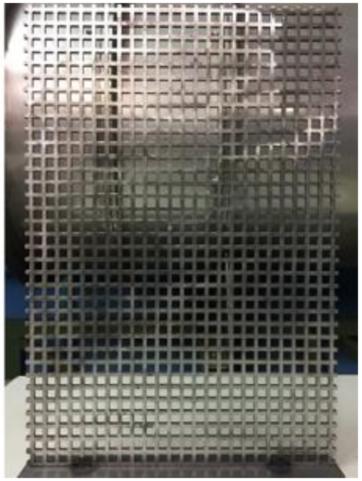

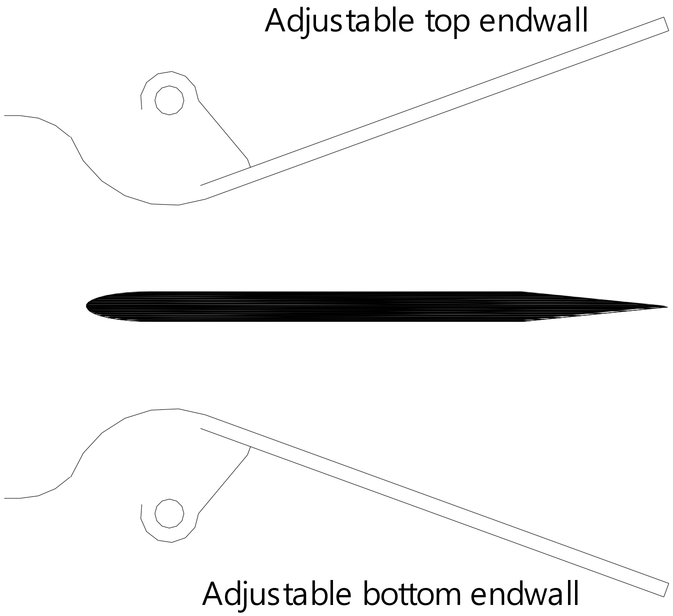

- ***Flat plate*** *installed within adjustable endwalls to control the pressure gradient. Upstream, different turbulence generating grids are adopted to test different free-stream turbulence intensity.*
    - *Boundary layer transition is experimentally characterized for variable* ***Reynolds numbers, free-stream turbulence intensities*** *and* ***adverse pressure gradients****.*

Test case and BCs

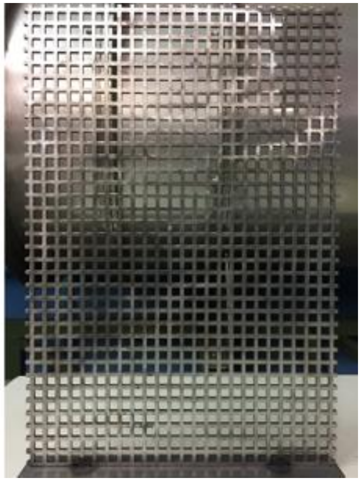

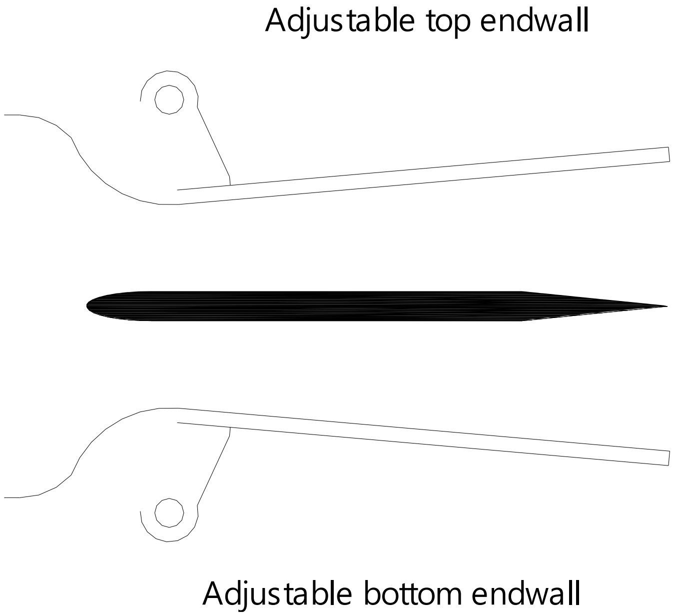

- ***Flat plate*** *installed within adjustable endwalls to control the pressure gradient. Upstream, different turbulence generating grids are adopted to test different free-stream turbulence intensity.*
    - *Boundary layer transition is experimentally characterized for variable **Reynolds numbers, free-stream turbulence intensities** and **adverse pressure gradients**.*

Test case and BCs

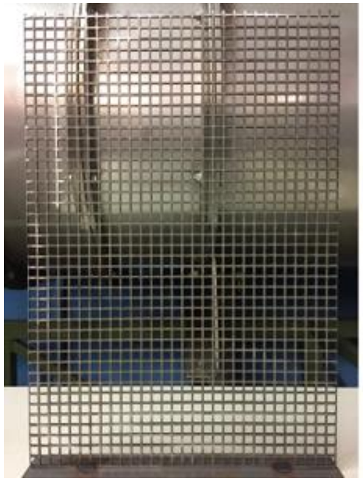

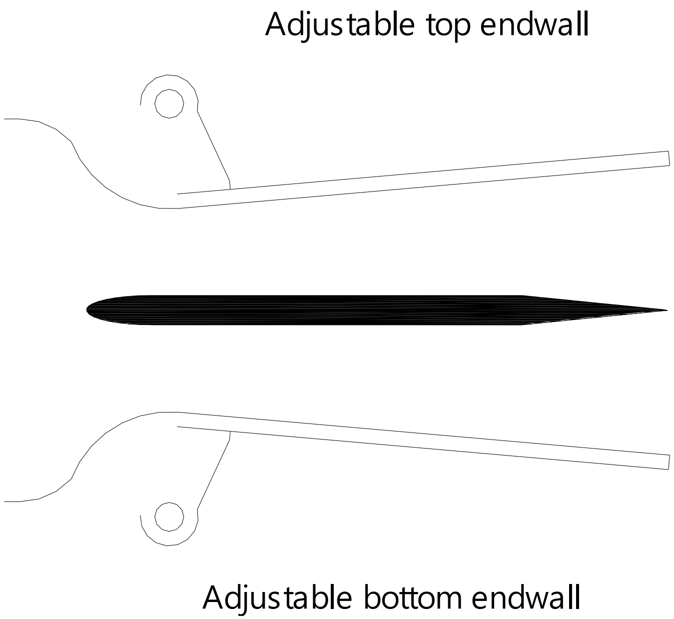

- ***Flat plate*** *installed within adjustable endwalls to control the pressure gradient. Upstream, different turbulence generating grids are adopted to test different free-stream turbulence intensity.*
    - *Boundary layer transition is experimentally characterized for variable* ***Reynolds numbers, free-stream turbulence intensities*** *and* ***adverse pressure gradients****.*

Test case and BCs

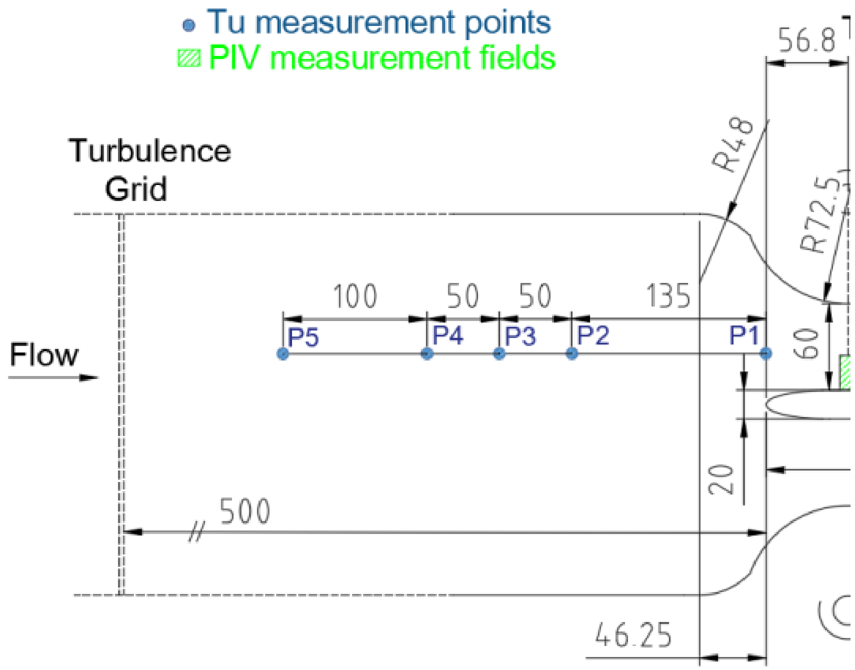

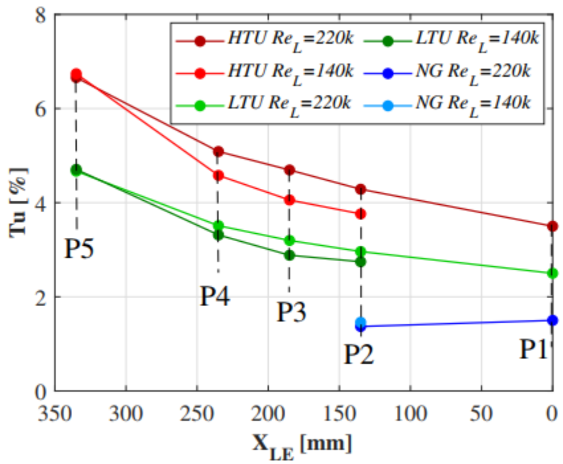

- ***Turbulence level*** *and* ***turbulence decay rate (****for properly set the* ***BCs in CFD*** *simulations are available)*

Measuring Techniques

Fast-Response **Particle Image Velocimetry (TR-PIV)** is used for the measurements on the plate

LASER SYSTEM:
- Double cavity ND: YLF pulsed laser LITRON-LDY300
- Energy 30 mJ per pulse at 527 nm

DOUBLE CAMERA:
- Dantec High-Sense digital camera
- 1280x1024 pixels cooled CCD matrix
- Pixel dimension 6.7 µm
- 12bit quantization
- Maximum frame rate in double frame mode: 3 kHz

POST PROCESSING
- 16x16 cross-correlation (50% overlap) and Gaussian sub-pixel interpolation
- **Spatial resolution = 0.41mm**

AQUIRED DATA
- $0.2 < x/L < 1$ (throat to end of the plate)
- 6000 PIV snapshot per flow condition
- Two acquisition frequencies: 0.3kHz and 1kHz

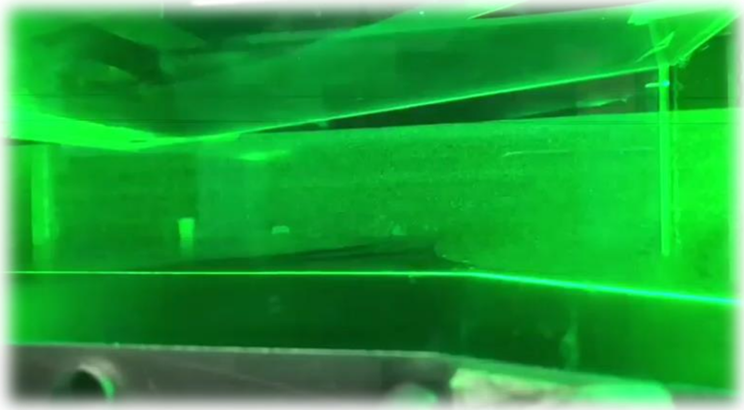

ESTIMATED ACCURACY
- **±3%** for the velocity in the free-stream
- **±6%** for the velocity in the BL region
- **±10-15%** for BL integral parameters

Database – first version acquired in the 2019

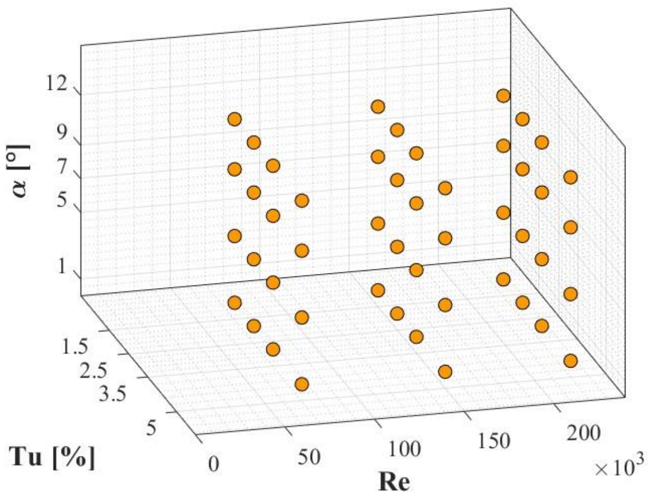

48 combination of flow conditions tested:

- Re = 70000, 150000, 220000
- Tu = 1.5%, 2.5%, 3.5%, 5%
- α = 12°, 9°, 5°, 1°

Simoni, D., et al. An accurate database on laminar-to-turbulent transition in variable pressure gradient flows. International Journal of Heat and Fluid Flow, 2019, 77: 84-97.

Database – first version acquired in the 2019

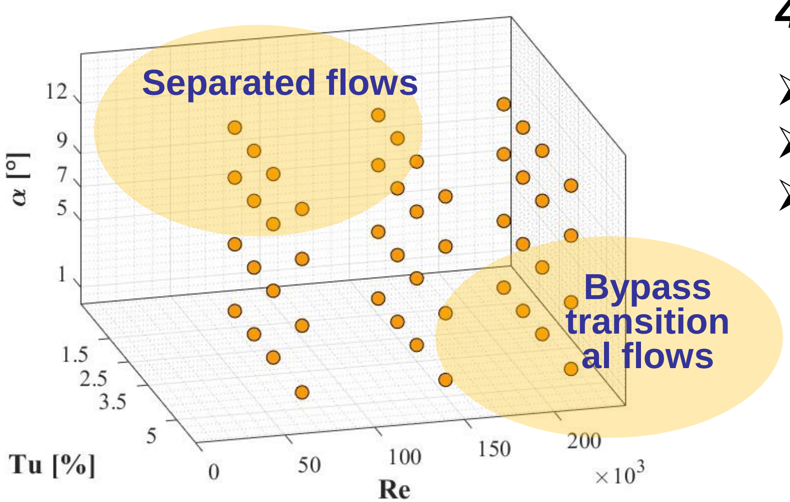

48 combination of flow conditions tested:

- Re = 70000, 150000, 220000
- Tu = 1.5%, 2.5%, 3.5%, 5%
- α = 12°, 9°, 5°, 1°

The range of parameter variation allows switching the transition process from a ***bypass*** *to* ***separation-induced type***

Simoni, D., et al. An accurate database on laminar-to-turbulent transition in variable pressure gradient flows. International Journal of Heat and Fluid Flow, 2019, 77: 84-97.

PIV statistics: effects of the Reynolds number

Streamwise velocity

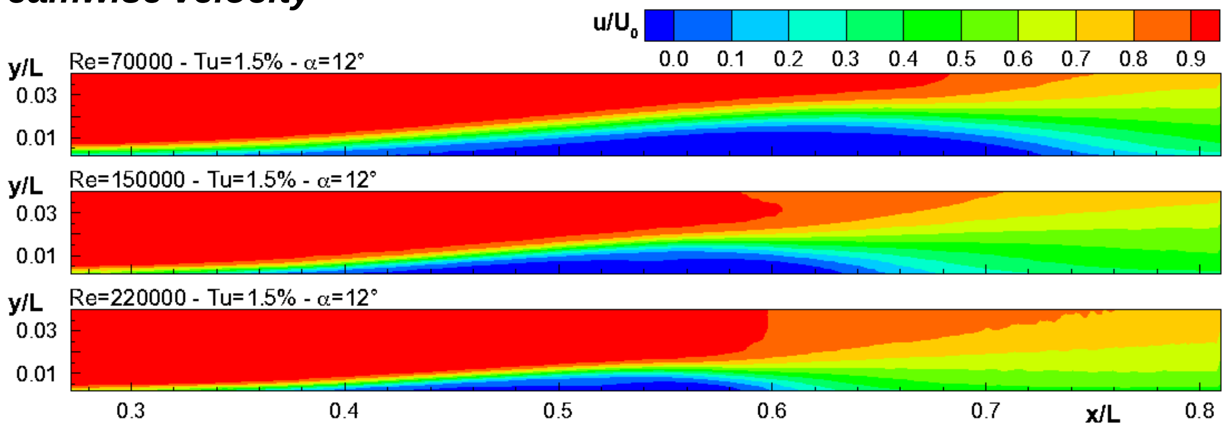

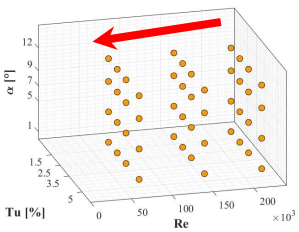

Rms of streamwise fluctuations

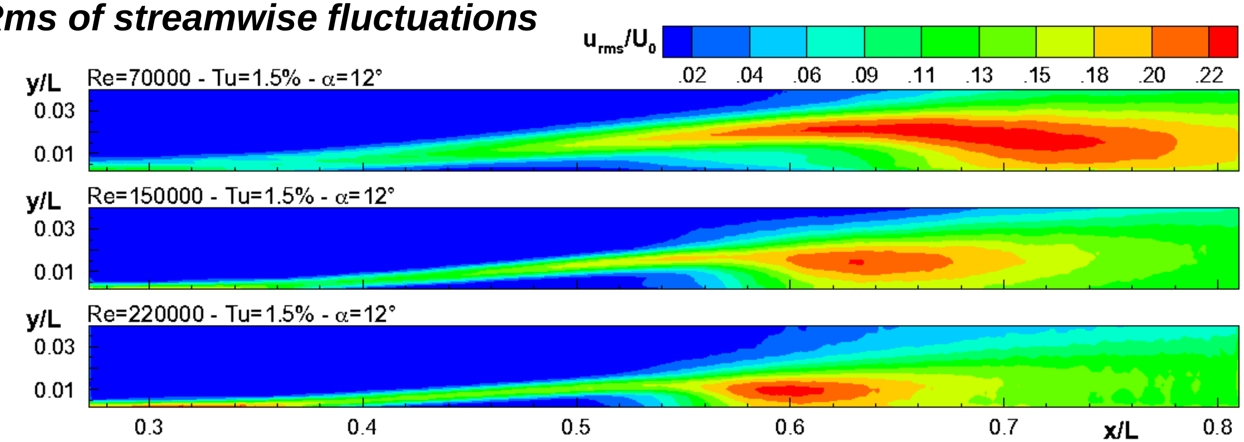

- *LSBs become shorter and thinner with increasing the Reynolds number and the BL thickness at separation significantly reduces.*

PIV statistics: effects of the Tu level

Streamwise velocity

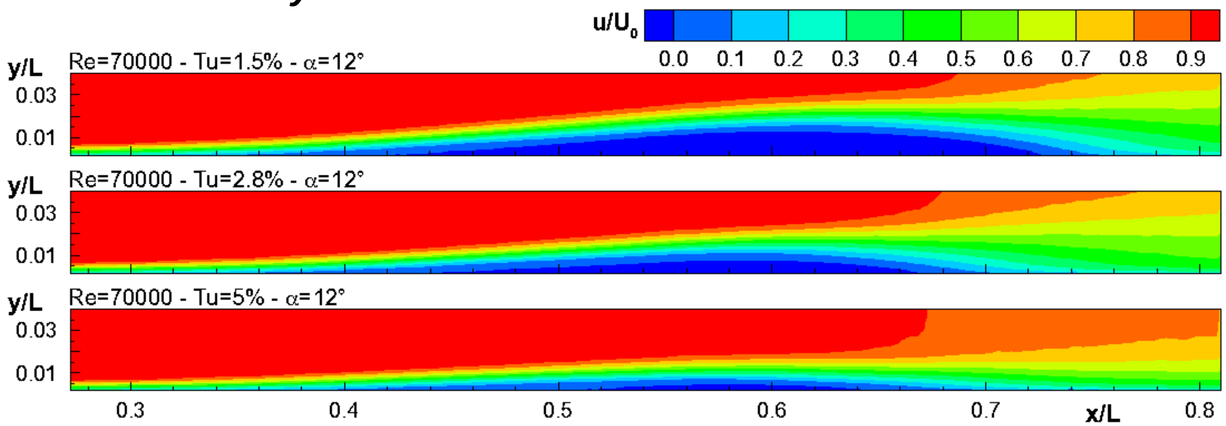

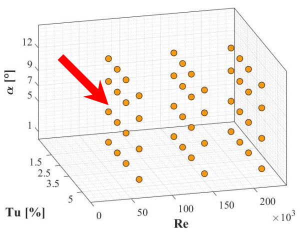

Rms of streamwise fluctuations

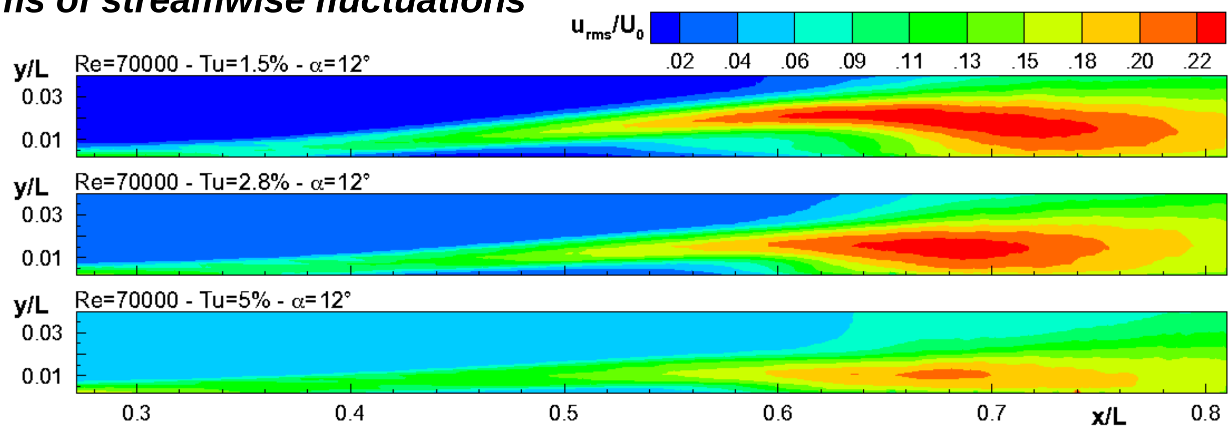

- *LSBs become shorter and thinner with increasing the Tu level while BL thickness at separation is unaffected by free-stream turbulence.*

PIV statistics: effects of the APG

Streamwise velocity

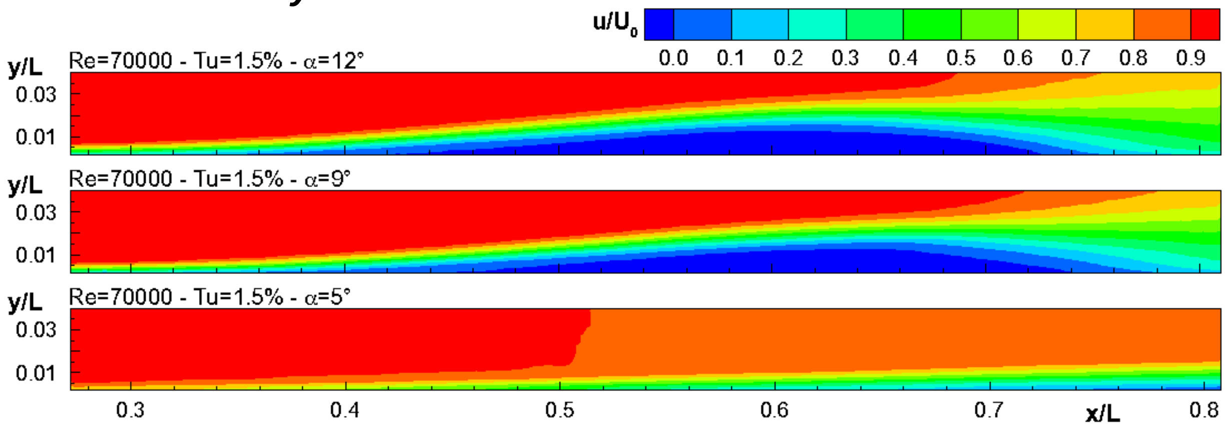

Rms of streamwise fluctuations

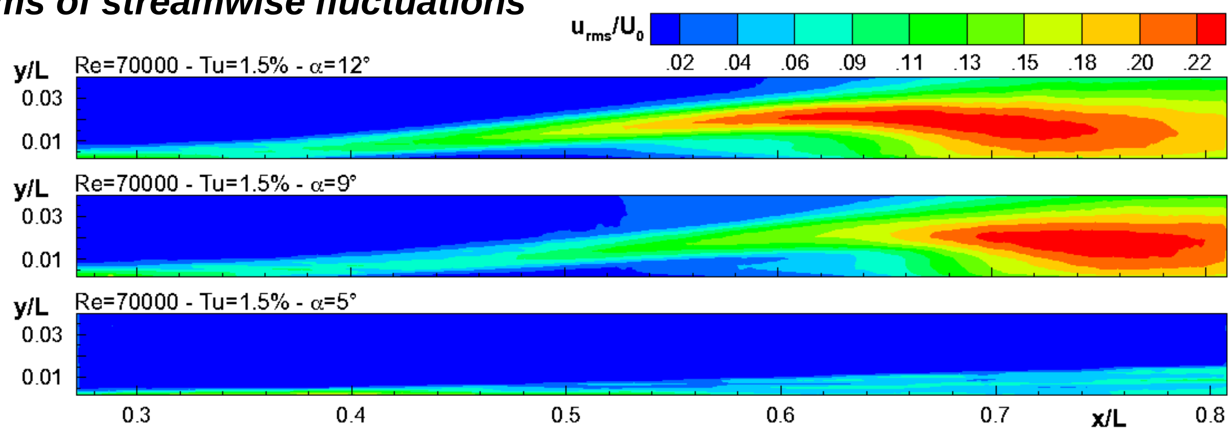

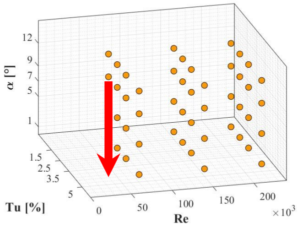

- *LSBs become longer and thinner with reducing the APG and separation moves downstream.*

Database – extended version 2022

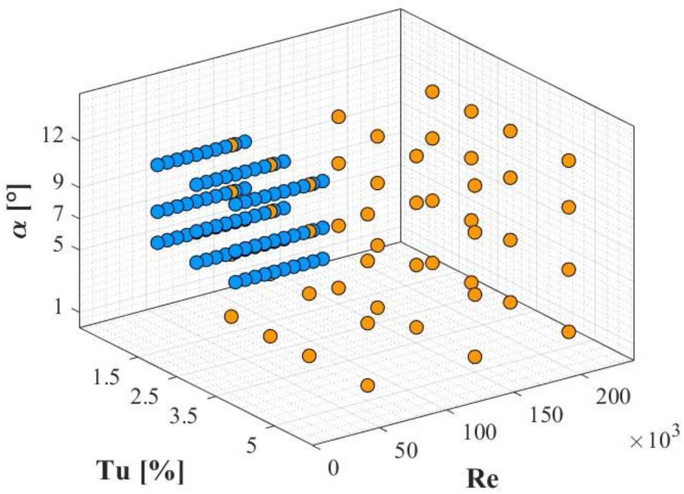

Additional 90 flow conditions acquired in the low Reynolds number region:

- ***15000 < Re < 80000***
- ***Tu = 1.5%, 2.5%, 3.5%***
- ***α = 12°, 9°, 7°***

Dellacasagrande, M., et al. "A data-driven analysis of short and long laminar separation bubbles." *Journal of Fluid Mechanics* 976 (2023)

Database – extended version 2022

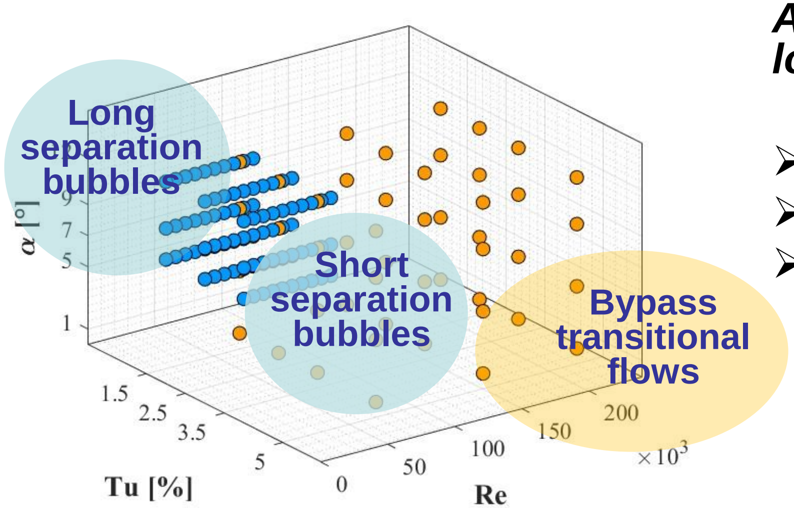

Additional 90 flow conditions acquired in the low Reynolds number region:

- ***15000 < Re < 80000***
- ***Tu = 1.5%, 2.5%, 3.5%***
- ***α = 12°, 9°, 7°***

*In the new database the flow **Re number** has been **finely reduced** to identify the **bursting process** of the laminar separation bubble, thus allowing to study both **short and long** separation bubbles*

Dellacasagrande, M., et al. "A data-driven analysis of short and long laminar separation bubbles." *Journal of Fluid Mechanics* 976 (2023)

Capturing of the bursting process

Reynolds number variation

Database 2019

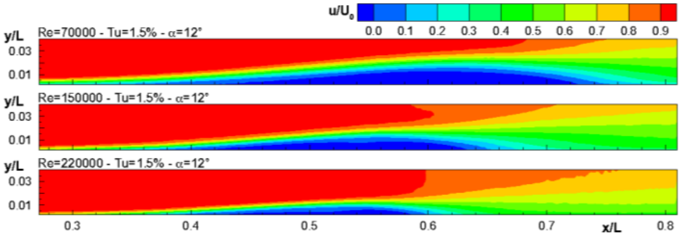

Capturing of the bursting process

Reynolds number variation

Database 2019

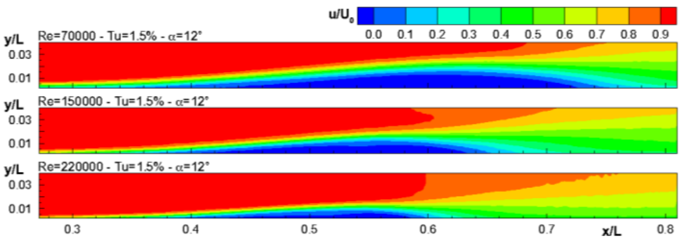

New Database

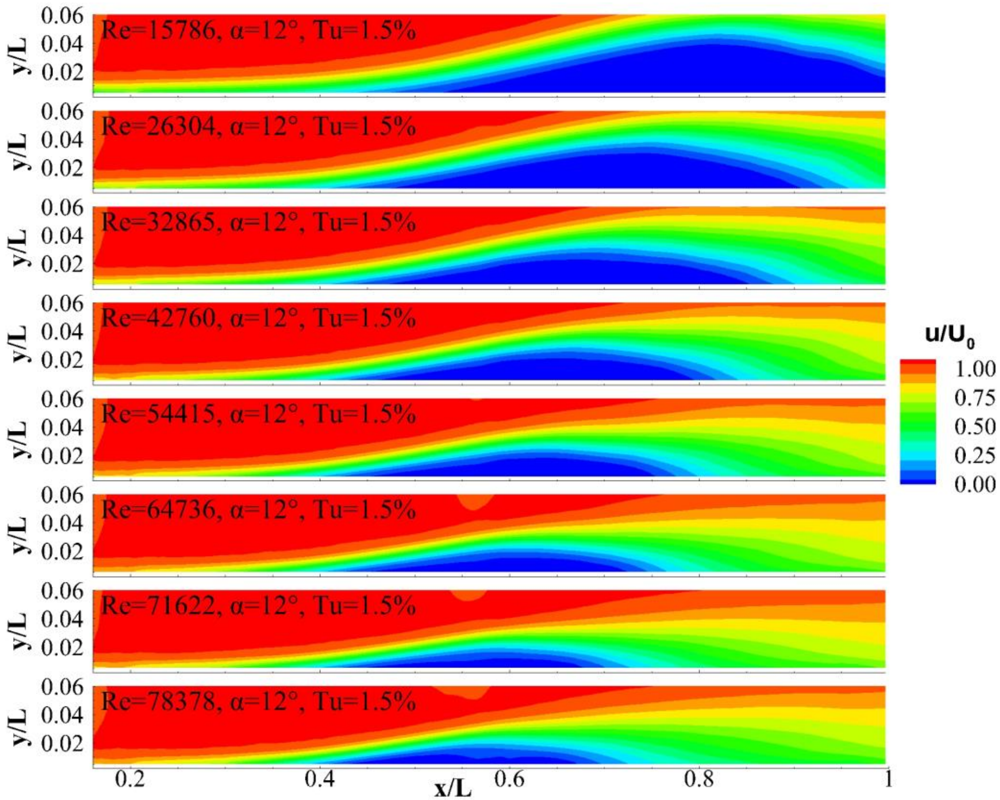

Capturing of the bursting process

Reynolds number variation

Database 2019

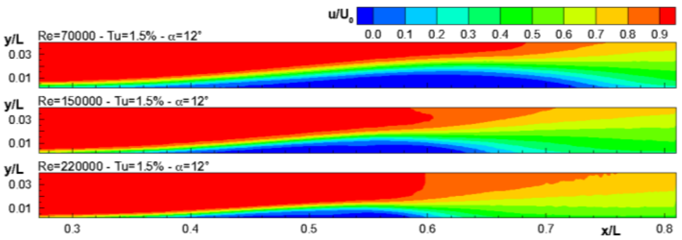

New Database

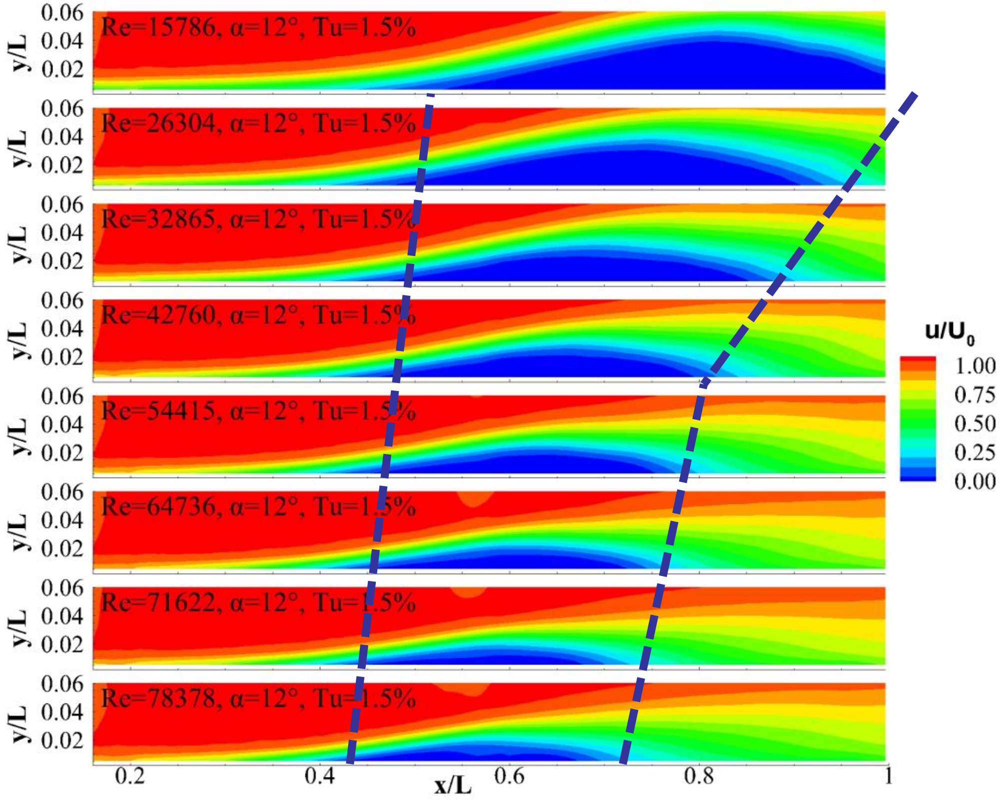

*We can clearly **capture** the **abrupt change** in the **bubble length** reducing the Re number **under the critical threshold***

Capturing of the bursting process

Reynolds number variation

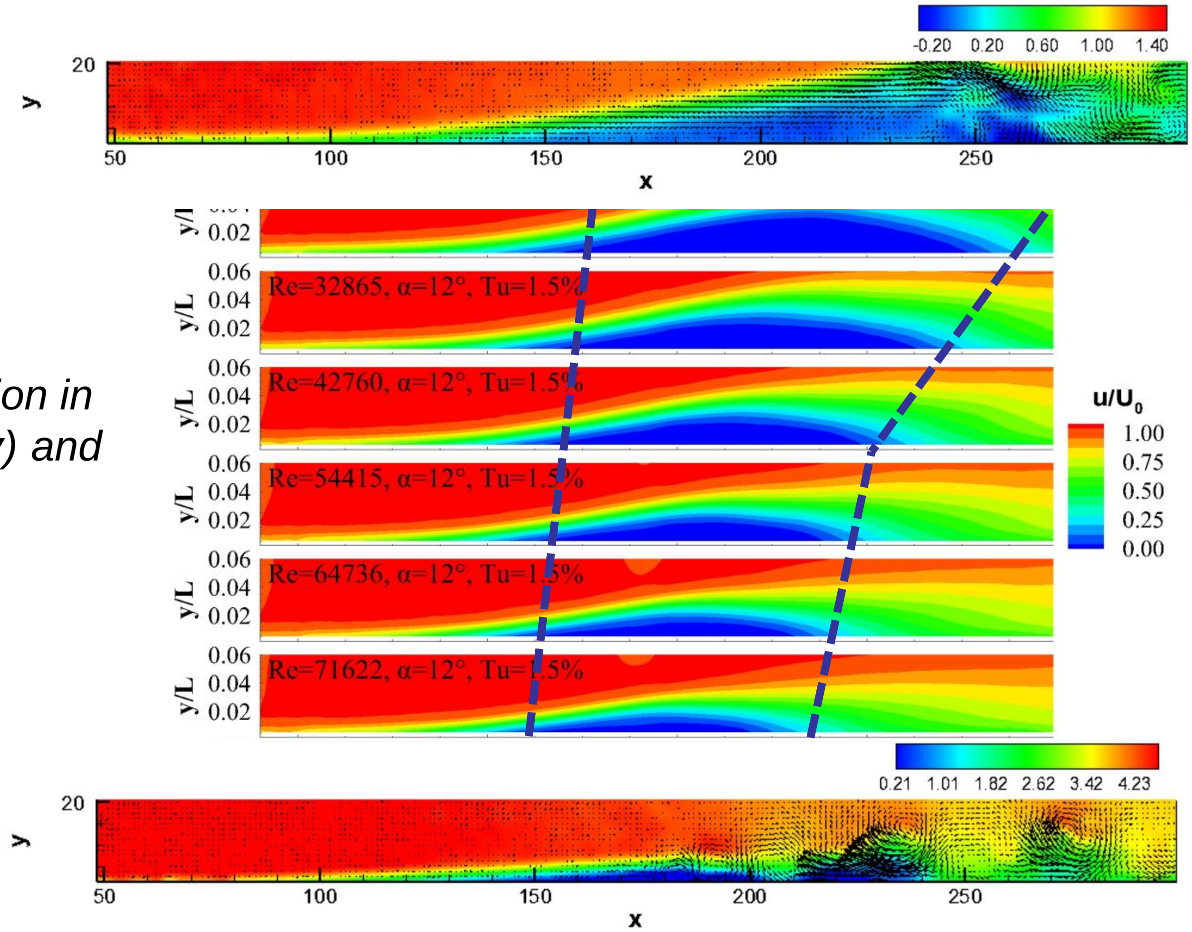

Different dynamics *lead to transition in the short (i.e. due to* ***KH instability****) and long (due to* ***absolute instability****) bubble type*

Example of possible learning procedures

Neural Networks does not *offer the possibility to highlight* ***weight of model ingredient*** *and their relation to flow physics*

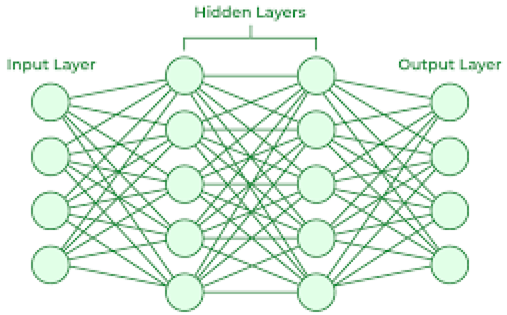

We prefer to adopt ***sparsity promoting*** *regression* ***tools to highlight flow features*** *mainly involved in the process*

$$\nu_t \; or \; \nu', \nu'', \nu''' = w_1 features_1 + w_2 features_2 + \cdots \ldots + w_{nm} features_n \; features_m$$

Learning Procedure for tuning

Elastic Net

- *Elastic Net is an **advanced technique** for **model learning**, proposed to improve Ordinary Least Square methods.*

- *In a common regression problem the target of the Elastic Net is finding the model coefficients $\hat{\beta}$ minimizing the Euclidean norm of the residuals, subject to both ℓ_1 and ℓ_2 **norm constrains** on the coefficients.*

$$\widehat{\boldsymbol{\beta}} = arg_{\beta} \min[|\boldsymbol{Y} - \boldsymbol{X}\,\boldsymbol{\beta}|^2 + \lambda_1|\boldsymbol{\beta}| + \lambda_2|\boldsymbol{\beta}|^2]$$

where:

  - $[\boldsymbol{Y}]_{NX1}$ *is the targeting function (N observations)*
  - $[\boldsymbol{X}]_{NXM}$ *is the Vandermonde matrix (N observations, M predictor functions)*
  - $[\boldsymbol{\beta}]_{MX1}$ *is the model coefficients vector*
  - λ_1 *and* λ_2 *are the penalization factors*

- *The introduction of the two penalization terms allows both **grouping of correlated variables** and **variable selection**. → Elastic Net can be used for the data driven **identification** of **simple and predictive models** for the terms of the closure equations.*

Learning Procedure for tuning

Lasso: matrix formulation

$$[X]\{\beta\} = \{\tau_{ij}\}$$

$$\begin{bmatrix} X_{1,1} & X_{2,1} & \cdots & X_{N,1} \\ X_{1,2} & X_{2,2} & \cdots & X_{1,2} \\ \vdots & \vdots & \cdots & \vdots \\ \vdots & \vdots & \vdots & \vdots \\ \vdots & \vdots & \vdots & \vdots \\ \vdots & \vdots & \cdots & \vdots \\ X_{1,\,ncond\cdot n_p} & X_{2,n_{cond}\cdot n_p} & \cdots & X_{N,ncond\cdot n_p} \end{bmatrix} \begin{bmatrix} \beta_1 \\ \beta_2 \\ \vdots \\ \vdots \\ \vdots \\ \vdots \\ \vdots \\ \beta_N \end{bmatrix} = \begin{bmatrix} \begin{bmatrix} \vdots \\ \tau_{ij} \\ \vdots \end{bmatrix}_{Re_1,Tu_1,AP_1} \\ \begin{bmatrix} \vdots \\ \tau_{ij} \\ \vdots \end{bmatrix}_{Re_1,Tu_1,AP_2} \\ \vdots \\ \vdots \\ \begin{bmatrix} \vdots \\ \tau_{ij} \\ \vdots \end{bmatrix}_{Re_L,Tu_M,AP_K} \end{bmatrix}$$

*The **predictors Xij** will be chosen from a **large library** of candidate functions (i.e. **flow features**)*

Learning Procedure for tuning

Lasso: matrix formulation

$$[X]\{\beta\} = \{\tau_{ij}\}$$

$$\begin{bmatrix} X_{1,1} & X_{2,1} & \cdots & X_{N,1} \\ X_{1,2} & X_{2,2} & \cdots & X_{1,2} \\ \vdots & \vdots & \cdots & \vdots \\ \vdots & \vdots & \vdots & \vdots \\ \vdots & \vdots & \vdots & \vdots \\ \vdots & \vdots & \cdots & \vdots \\ X_{1,n_{cond}\cdot n_p} & X_{2,n_{cond}\cdot n_p} & \cdots & X_{N,ncond\cdot n_p} \end{bmatrix} \begin{bmatrix} \beta_1 \\ \beta_2 = 0 \\ \vdots \\ \vdots \\ \vdots \\ \vdots \\ \vdots \\ \beta_N \end{bmatrix} = \begin{bmatrix} \begin{bmatrix} \vdots \\ \tau_{ij} \\ \vdots \end{bmatrix}_{Re_1,Tu_1,AP_1} \\ \begin{bmatrix} \vdots \\ \tau_{ij} \\ \vdots \end{bmatrix}_{Re_1,Tu_1,AP_2} \\ \vdots \\ \vdots \\ \begin{bmatrix} \vdots \\ \tau_{ij} \\ \vdots \end{bmatrix}_{Re_L,Tu_M,AP_K} \end{bmatrix}$$

Practically, flow features with a coefficient below a fixed threshold will be discharged

Learning Procedure for tuning

Bayesian Lasso

Sparse Bayesian Learning *is used to obtain sparse models from data. Given a set of* N *samples, the observable* $\boldsymbol{t}$ *(i.e., the* ***anisotropy tensor*** $\boldsymbol{a}_{ij}$*) is modelled as a linear combination of predictors* $\boldsymbol{C}(\boldsymbol{x})$ *and coefficients* $\boldsymbol{w}$ *plus an additional noise* $\boldsymbol{\varepsilon}$*:*

$$\boldsymbol{t} = \boldsymbol{C}(\boldsymbol{x})\,\boldsymbol{w} + \boldsymbol{\varepsilon}$$

Regression problem is approached in the ***Bayesian framework****, where a* ***Gaussian probability distribution is assigned to the observations****, given the model:*

$$p(\boldsymbol{t}|\boldsymbol{w},\sigma_n) = N(\boldsymbol{t};\, \boldsymbol{C}\boldsymbol{w}, \sigma_n^2\boldsymbol{I}) = (2\pi\sigma_n^2)^{-\frac{N}{2}} \exp\left(-\frac{1}{2\sigma_n^2}||\boldsymbol{t}-\boldsymbol{C}\boldsymbol{w}||^2\right)$$

Learning Procedure for tuning

Bayesian Lasso

Sparse Bayesian Learning *is used to obtain sparse models from data. Given a set of N samples, the observable* ***t*** *(i.e., the* ***anisotropy tensor*** *$\boldsymbol{a_{ij}}$) is modelled as a linear combination of predictors $\boldsymbol{C}(\boldsymbol{x})$ and coefficients $\boldsymbol{w}$ plus an additional noise $\boldsymbol{\varepsilon}$:*

$$\boldsymbol{t} = \boldsymbol{C}(\boldsymbol{x})\,\boldsymbol{w} + \boldsymbol{\varepsilon}$$

Regression problem is approached in the ***Bayesian framework****, where a* ***Gaussian probability distribution is assigned to the observations****, given the model:*

$$p(\boldsymbol{t}|\boldsymbol{w},\sigma_n) = N(\boldsymbol{t};\ \boldsymbol{C}\boldsymbol{w},\sigma_n^2\boldsymbol{I}) = (2\pi\sigma_n^2)^{-\frac{N}{2}}\exp\left(-\frac{1}{2\sigma_n^2}||\boldsymbol{t}-\boldsymbol{C}\boldsymbol{w}||^2\right)$$

Sparsity is promoted by two hierarchical prior assumptions:

- ***A normal probability distribution*** *with zero mean and adjustable dispersions α_i* ***is assumed for the model coefficients:***

$$p(\boldsymbol{w}|\alpha) = N(\boldsymbol{w};\ 0,\boldsymbol{A}^{-1}),\quad \boldsymbol{A} = diag(\boldsymbol{\alpha})$$

- The **dispersions $\boldsymbol{\alpha_i}$ are assumed** to follow a **Laplace probability distribution:**

$$p(\boldsymbol{\alpha}) = \prod_i \frac{\lambda}{2}exp(-\frac{\lambda}{2\alpha_i})$$

Learning Procedure for tuning

Bayesian Lasso

Sparse Bayesian Learning *aims at defining the* ***model coefficients/hyperparameters*** $\{\boldsymbol{w}, \boldsymbol{\alpha}, \boldsymbol{\sigma_n^2}\}$ *allowing the definition of* ***parsimonious models.*** *To this end, the maximum of* ***posterior joint probability*** $\boldsymbol{p(w, \alpha, \sigma_n|t)}$ ***is searched****, following the method proposed in [1]:*

$$p(\boldsymbol{w}, \alpha, \sigma_n|\boldsymbol{t}) = \underbrace{p(\boldsymbol{w}|\boldsymbol{t}, \alpha, \sigma_n)}\ \underbrace{p(\alpha, \sigma_n|\boldsymbol{t})}$$

The maximum of $p(\boldsymbol{w}|\boldsymbol{t}, \boldsymbol{\alpha}, \sigma_n)$*, i.e., the posterior distribution of the coefficients, provides the* ***best value of*** w ***given*** α ***and*** $\boldsymbol{\sigma_n}$***:***

$$\begin{cases} \boldsymbol{\Sigma} = \left(\boldsymbol{A} + \sigma_n^{-2}\boldsymbol{C}^T\boldsymbol{C}\right)^{-1} \\ \boldsymbol{\mu} = \sigma_n^{-2}\Sigma\boldsymbol{C}^T\boldsymbol{t} \end{cases}$$

The probability for $p(\boldsymbol{\alpha}, \boldsymbol{\sigma_n}|\boldsymbol{t})$ *(multi-dimensional Dirac function) leads to the definition of the* ***marginal likelihood*** $\boldsymbol{L_{II}}$ *[2] as the cost function used for setting* $\boldsymbol{\alpha}$ ***and*** $\boldsymbol{\sigma_n}$***:***

$$\begin{cases} \alpha_i^{new} = \frac{1+\sqrt{1+8\lambda(\mu_i^2+\Sigma_{ii})}}{2(\mu_i^2+\Sigma_{ii})} \\ (\sigma_n^2)^{new} = \frac{||t-C\mu||^2}{N} \end{cases}$$

The sparsity term $\boldsymbol{\lambda}$ *is finally evaluated* ***by cross-validation*** *(and/or* ***validation with respect to unseen flow cases****)*

Tipping, Michael E. "Sparse Bayesian learning and the relevance vector machine." *Journal of machine learning research* Jun (2001): 211-244.

Balakrishnan, Suhrid, and David Madigan. "Priors on the variance in sparse Bayesian learning: the demi-Bayesian lasso." (2010): 346-359.

Learning Procedure for tuning

Bayesian Lasso

*Some examples of **retained** and **skipped** terms*

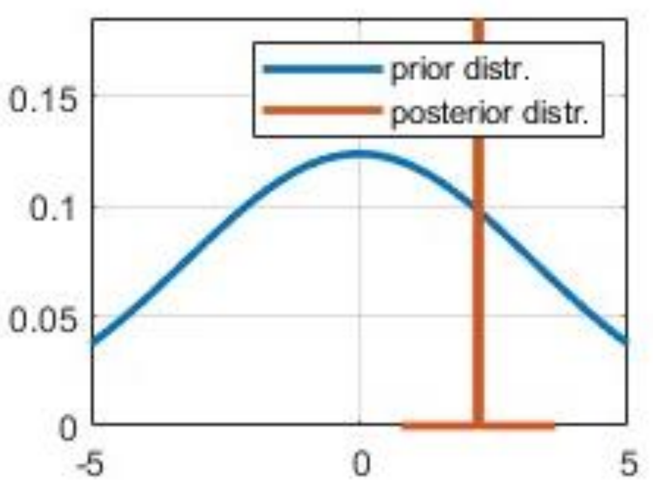

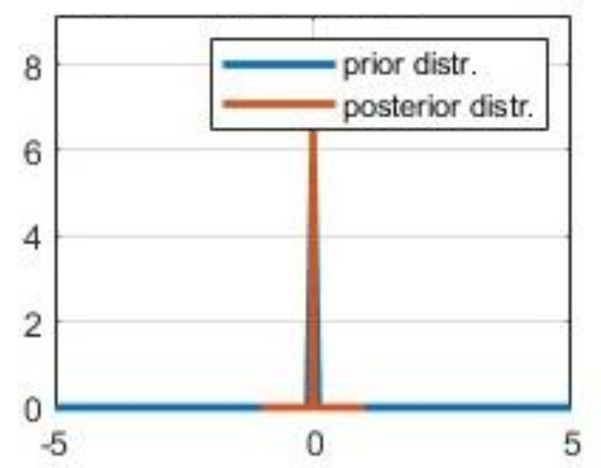

Retained terms have a prior distribution with large variance

Skipped terms have a prior distribution close to a Dirac function

Learning Procedure for tuning

Bayesian Lasso

***Retained terms** may exhibit **low or large variance** (i.e. confident level)*

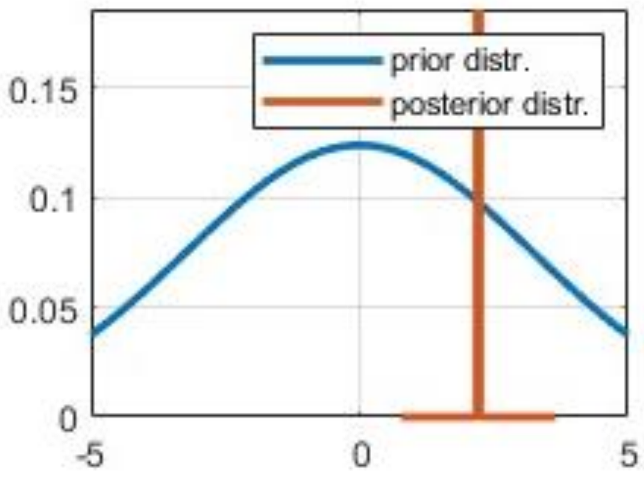

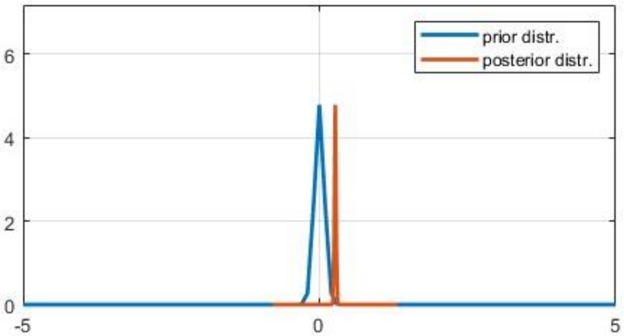

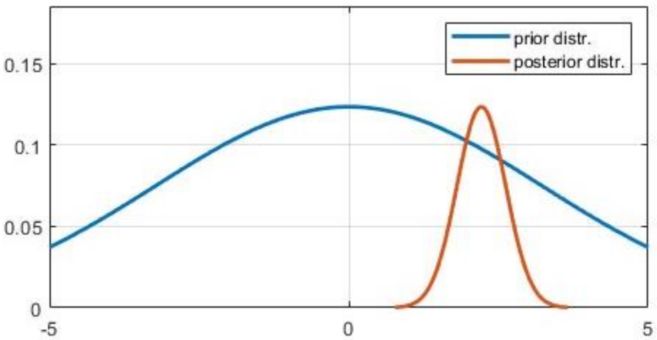

*Coefficients with **small variance** are **more "sure"** than the other*

Results and tuned models

- ***γ-Reθ*** *model*
- ***LKE*** *(Laminar Kinetic energy) model*
- ***Algebraic*** *models*

γ-Re$_\theta$ transition model

- *The **γ-Re$_\theta$ models** involve **two additional equations**, with respect to a classic K-ε approach:*

  *_A differential equation for the **intermittency function** γ*

  *_An algebraic equation for the **transition onset position** Re$_\theta$*

- *The **structure** of the model is:*

$$
\begin{cases}
\dfrac{D\overline{\boldsymbol{U}}}{Dt} = -\dfrac{1}{\rho}\boldsymbol{\nabla}\left(\overline{p} + \dfrac{2}{3}K\right) + (\nu + \nu_T)\boldsymbol{\nabla}^2\overline{\boldsymbol{U}} \\
\dfrac{DK}{Dt} = P_K + D_K - \varepsilon \\
\dfrac{D\varepsilon}{Dt} = P_\varepsilon + D_\varepsilon - \varepsilon_\varepsilon \\
\dfrac{D\gamma}{Dt} = \boxed{P_\gamma} + D_\gamma - \varepsilon_\gamma \\
\boxed{Re_{\theta\_st} = f(Tu, \lambda_\theta)}
\end{cases}
$$

*Need to be **tuned by empirical correlations**.*

*where: the equations are related by means of the **dimensional relationship**:* $\nu_T = C_\mu \dfrac{K^2}{\varepsilon}\gamma$

Data reduction for transition modelling (γ-Re$_\theta$)

- *A procedure for the* ***computation of the intermittency function γ*** *has been implemented based on a* ***coherent structures recognition technique****.*

- *The* ***Wavelet Transform*** *has been adopted as* ***events recognition technique*** *to detect coherent structures responsible for transition.*

Wavelet Transform ***definition****:*

$$w(x,s) = \int f(x') \frac{1}{\sqrt{s}} \psi^* \left(\frac{x' - x}{s} \right) dx'$$

where: x *spatial position*

s *length scale*

ψ^* *mother function*

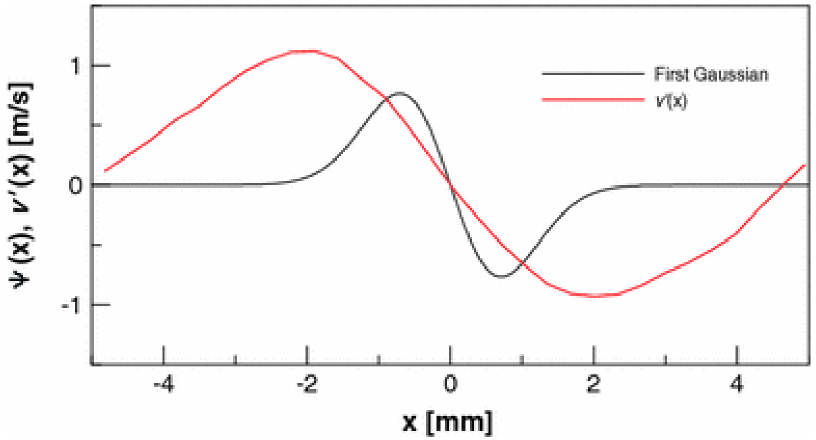

Data reduction for transition modelling (γ-Re_θ)

- *The **energy spectrum** can be computed as:*

$$E(x,y,s)=\frac{\sqrt{\left[w(s)_{1,2}w(s)^{*}{}_{1,2}\right]\left[w(s)_{2,1}w(s)^{*}{}_{2,1}\right]}}{s}$$

$$e(s)=\iint E(x,y,s)dxdy$$

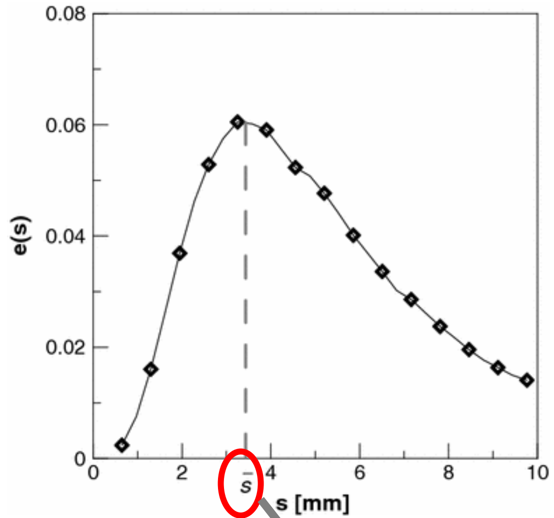

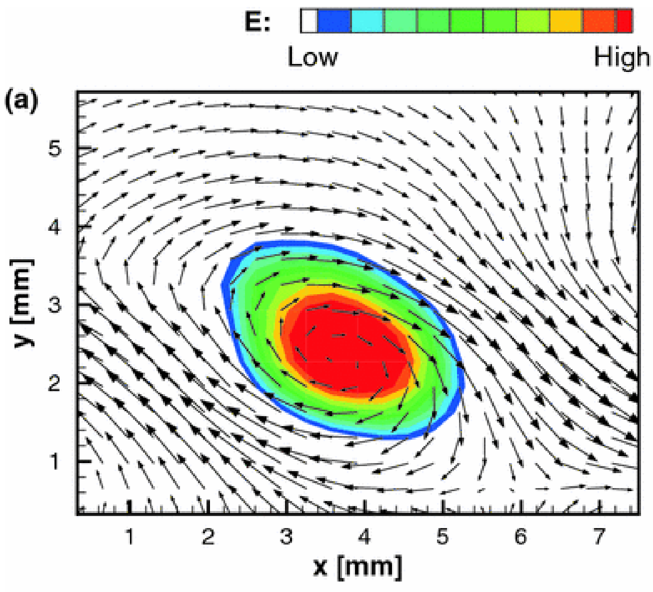

- *Choosing the length scale $\overline{s}$ **maximizing the energy**, the spatial distribution of the wavelet spectral energy clearly **highlights vortical structures into the flow**.*

Data reduction for transition modelling (γ-Re_θ)

Vortices recognition

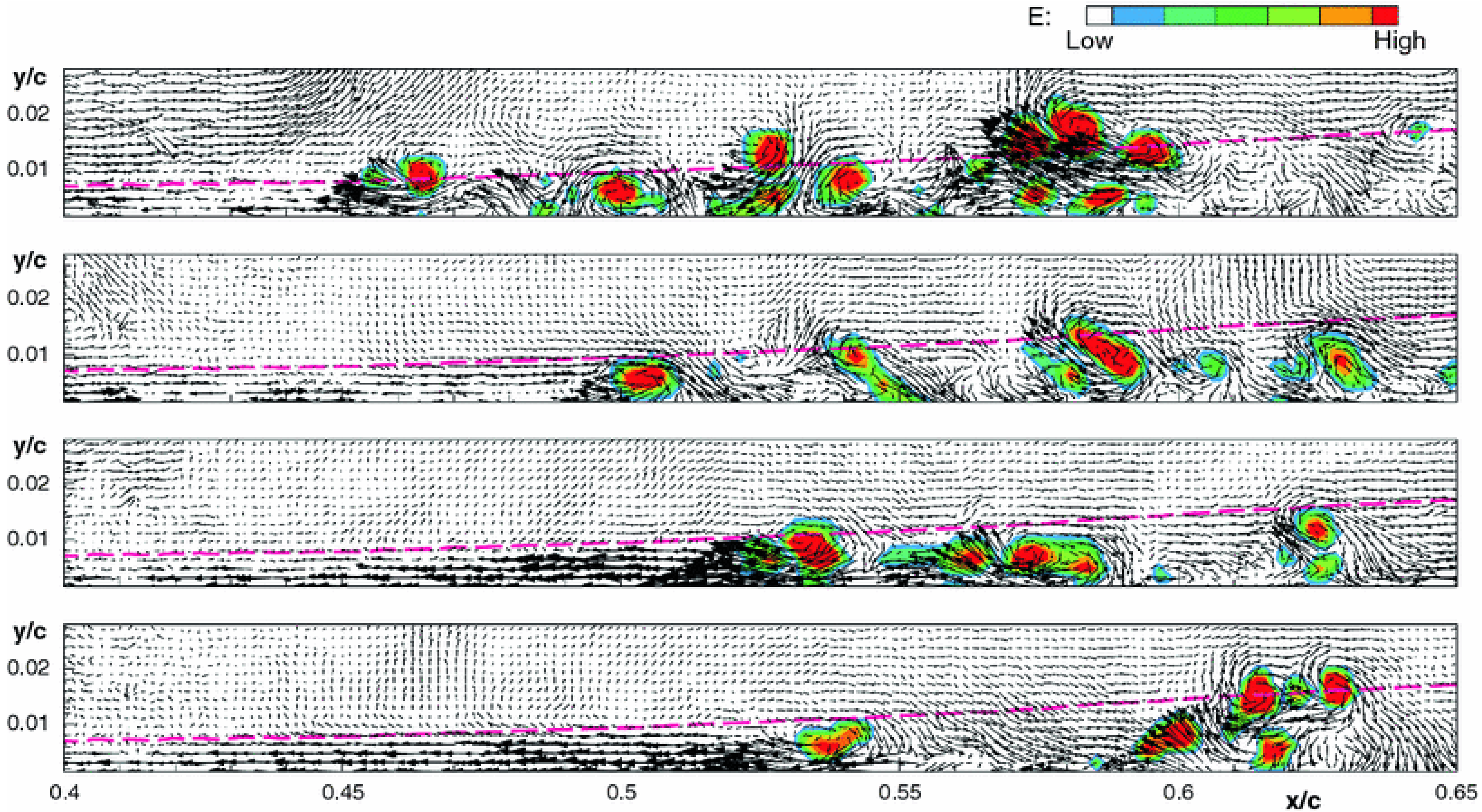

- *Vortices occurring in the BL are* ***well captured*** *by the* ***Wavelet based procedure***

Data reduction for transition modelling (γ-Re$_\theta$)

Computing the intermittency function γ

- *Integrating over the variable y:* $$\tilde{e}(x,\bar{s}) = \int E(x,y,\bar{s})dy$$
- *Introducing a* ***counter function*** n, *considering the sum over all the* N_y *PIV snapshots*

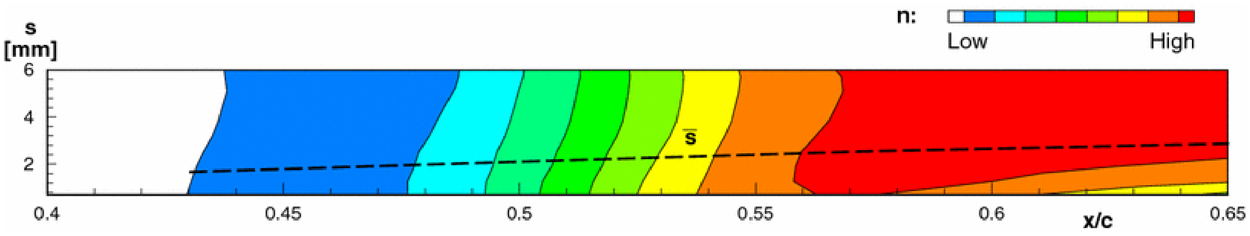

- *The* ***intermittency function γ*** *is derived from the data:*

$$\boxed{\gamma(x) = \frac{n(x,\bar{s})}{\max(n)}}$$

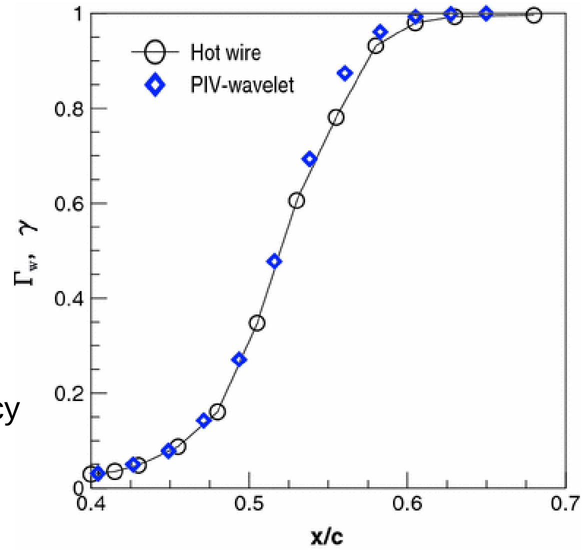

Simoni D., Lengani D., Guida R., “A wavelet-based intermittency detection technique from PIV investigations in transitional boundary layers”, Experiments in Fluids, Vol. 57(9), pp. 145, 2016

Data reduction for transition modelling (γ-Re_θ)

- ***Intermittency function γ for different flow condition** (Re, Tu)*

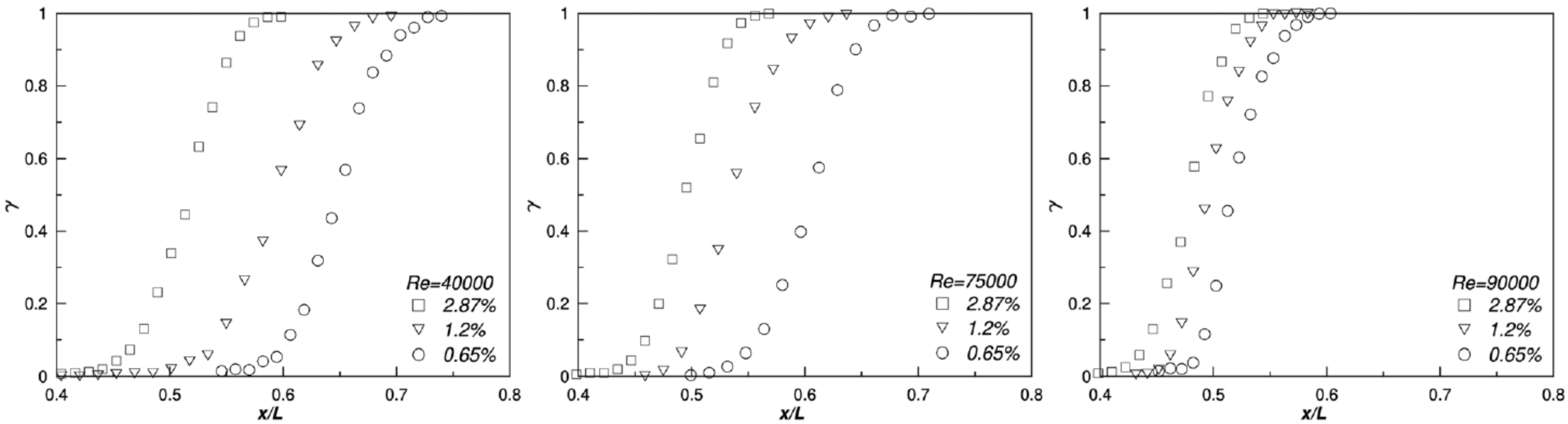

- *The **computation of γ** directly provides for every flow condition:*
  - *The **transition onset** location (x_t/L)*
  - *The **transition end** location (x_T/L)*
  - *The **turbulent spot production rate** $(\hat{n}\sigma)$*

Empirical correlations for transition (γ-Reθ)

- ***RANS*** *simulations based on γ-Reθ transition models* ***require closure terms*** *providing the* ***transition onset*** *and the* ***spot production rate***

- *Thanks to the previous observations,* ***empirical correlations*** *can be obtained, using the least square best fitting:*
  - *For the* ***transition onset Reynolds number****:* $$Re_{st} = C\frac{{Re_\theta}^n}{Tu^m}$$
  - *For the* ***turbulent spot production rate****:* $$\hat{n}\sigma = \frac{C'}{{Re_\theta}^{n'}}$$

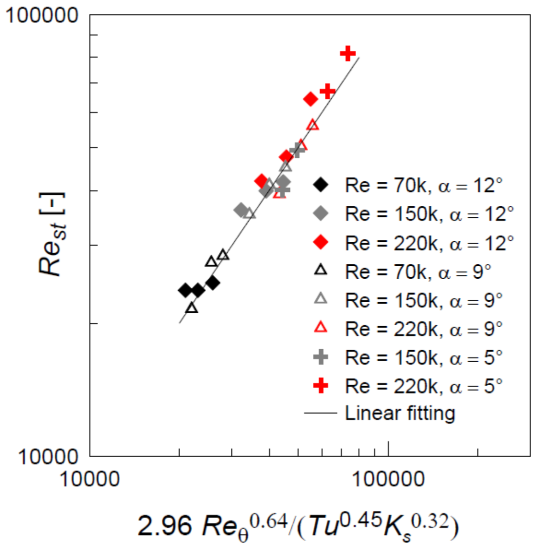

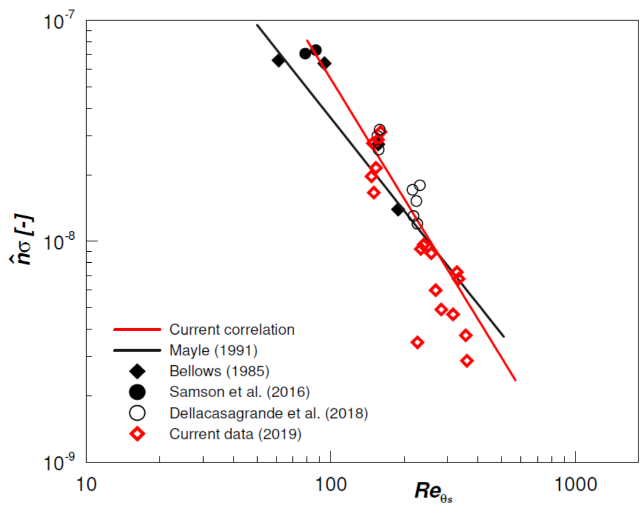

Dellacasagrande, Matteo et al. Correlations for the Prediction of Intermittency and Turbulent Spot Production Rate in Separated Flows. Journal of Turbomachinery, 2019.

Results and tuned models

- ***γ-Re$_\theta$*** *model*
- ***LKE*** *(Laminar Kinetic energy) model*
- ***Algebraic*** *models*

Laminar-Kinetic Energy transition model

- *The **structure** of the LKE model:*

$$\begin{cases} \dfrac{D\overline{\boldsymbol{U}}}{Dt} = -\dfrac{1}{\rho}\boldsymbol{\nabla}\left(\overline{p} + \dfrac{2}{3}K\right) + (\nu + \nu_T)\boldsymbol{\nabla}^2\overline{\boldsymbol{U}} \\ \dfrac{DK_L}{Dt} = P_{K_L} + D_{K_L} - R - \varepsilon \\ \dfrac{DK_T}{Dt} = P_{K_T} + D_{K_T} + R - \varepsilon \\ \dfrac{D\varepsilon}{Dt} = P_\varepsilon + D_\varepsilon - \varepsilon_\varepsilon \end{cases}$$

*where the equations are related by means of a **relationship**:* $\nu_T = \nu_T(K_L, K_T, \varepsilon)$

- *Based on the **Hussain and Reynolds triple decomposition,** K_L and K_T can be defined as:*

$$\frac{D(\frac{1}{2}\overline{\tilde{u}_i\tilde{u}_i})}{Dt} = \cdots + (-\overline{\tilde{u}_i\tilde{u}_i})\frac{\partial \overline{U}_i}{\partial x_j} - \overline{(-\langle u_i'u_j'\rangle)\frac{\partial \tilde{u}_i}{\partial x_j}} - \frac{1}{2Re}\overline{\left(\frac{\partial \tilde{u}_j}{\partial x_i} + \frac{\partial \tilde{u}_i}{\partial x_j}\right)\left(\frac{\partial \tilde{u}_j}{\partial x_i} + \frac{\partial \tilde{u}_i}{\partial x_j}\right)}$$

$$\frac{D(\frac{1}{2}\overline{u_i'u_i'})}{Dt} = \cdots + (-\overline{u_i'u_j'})\frac{\partial \overline{U}_i}{\partial x_j} + \overline{(-\langle u_i'u_j'\rangle)\frac{\partial \tilde{u}_i}{\partial x_j}} - \frac{1}{2Re}\overline{\left(\frac{\partial u_j'}{\partial x_i} + \frac{\partial u_i'}{\partial x_j}\right)\left(\frac{\partial u_j'}{\partial x_i} + \frac{\partial u_i'}{\partial x_j}\right)}$$

Laminar-Kinetic Energy transition model

- *The **structure** of the LKE model:*

$$\begin{cases} \dfrac{D\overline{\boldsymbol{U}}}{Dt} = -\dfrac{1}{\rho}\boldsymbol{\nabla}\left(\overline{p} + \dfrac{2}{3}K\right) + (\nu + \nu_T)\boldsymbol{\nabla}^2\overline{\boldsymbol{U}} \\ \dfrac{DK_L}{Dt} = P_{K_L} + D_{K_L} - R - \varepsilon \\ \dfrac{DK_T}{Dt} = P_{K_T} + D_{K_T} + R - \varepsilon \\ \dfrac{D\varepsilon}{Dt} = P_\varepsilon + D_\varepsilon - \varepsilon_\varepsilon \end{cases}$$

*where the equations are related by means of a **relationship**:* $\nu_T = \nu_T(K_L, K_T, \varepsilon)$

- *Based on the **Hussain and Reynolds triple decomposition,** K_L and K_T can be defined as:*

$$\boldsymbol{u} = \overline{\boldsymbol{U}} + \widetilde{\boldsymbol{u}} + \boldsymbol{u}'$$

where: $\overline{\boldsymbol{U}}$ *is the average value describing the mean flow.*

$\widetilde{\boldsymbol{u}}$ *is the deterministic part of the fluctuations describing the laminar flow*

$\boldsymbol{u}'$ *is the stochastic part of the fluctuations describing the turbulent flow*

POD as a tool for scale separation

- ***POD*** *can be adopted to* ***distinguish*** *between* ***laminar*** *(coherent) and* ***turbulent*** *(stochastic) fluctuations*

$$u(x,y,t_i) = \sum_{k=1}^{N} \chi^k(t_i)\varphi^k(x,y)$$

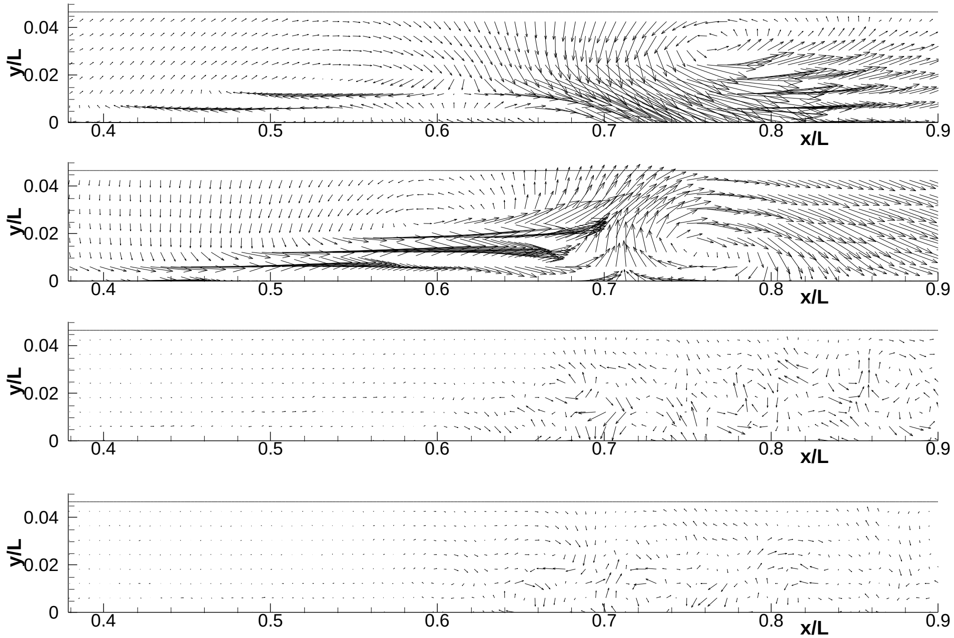

Mode 1

Mode 2

Mode 50

Mode 51

- *Coherent modes ($k < k^*$)* → *Laminar (coherent) scales*
- *Stochastic modes ($k > k^*$)* → *Turbulent scales*

Data reduction for transition modelling (LKE)

Terms expressed by POD

Exact definition
(from Hussein and Reynolds equations)

Fragment definition from POD

$$K_L = \frac{1}{2}\sum_i \overline{\tilde{u}_i\tilde{u}_i} \longrightarrow K_L = \frac{1}{2}\sum_{t=1}^{k^*} \varphi_i^{(t)}\varphi_i^{(t)}$$

$$K_T = \frac{1}{2}\sum_i \overline{u_i'u_i'} \longrightarrow K_T = \frac{1}{2}\sum_{t=k^*+1}^{N} \varphi_i^{(t)}\varphi_i^{(t)}$$

$$P_{K_L} = \overline{\tilde{u}_i\tilde{u}_j}\frac{\partial \bar{U}_i}{\partial x_j} \longrightarrow P_{K_L} = \sum_{t=1}^{k^*} \varphi_i^{(t)}\varphi_j^{t)} \cdot \frac{\partial \bar{U}_i}{\partial x_j}$$

$$P_{K_T} = \overline{u_i'u_j'}\frac{\partial \bar{U}_i}{\partial x_j} \longrightarrow P_{K_T} = \sum_{t=k^*+1}^{N} \varphi_i^{(t)}\varphi_j^{t)} \cdot \frac{\partial \bar{U}_i}{\partial x_j}$$

$$R = \overline{< u_i'u_j' > \frac{\partial \tilde{u}_i}{\partial x_j}} \longrightarrow R = \overline{\left(\sum_{k=k^*+1}^{N} \varphi_i^{(k)}\chi^{(k)} \sum_{k=k^*+1}^{N} \varphi_j^{(k)}\chi^{(k)}\right)\frac{\partial \sum_{k=1}^{k^*} \varphi_i^{(k)}\chi^{(k)}}{\partial x_j}}$$

Model definition

Modelling: *example of the model for the laminar energy production term.*

$$P_{K_L} = f_1 \frac{K_L^2}{\mathbf{e}} \left(\frac{\partial \overline{U}}{\partial x} \right)^2 + f_2 \frac{K_L^2}{\mathbf{e}} \left(\frac{\partial \overline{U}}{\partial y} \right)^2 + f_3 \frac{K_L^2}{\mathbf{e}} \left(\frac{\partial \overline{V}}{\partial x} \right)^2 + f_4 \frac{K_L^2}{\mathbf{e}} \left(\frac{\partial \overline{V}}{\partial y} \right)^2$$

where $f_1 - f_4 = f\{Re, Tu, |S|\}$ *are* ***blending functions*** *(second order polynomials) of the most influencing parameters affecting transition: the* ***Reynolds number****, the* ***free-stream turbulence level and the shear invariant****.*

- *Similarly, for the other terms:*

Laminar energy production term	$P_{K_L} = P_{K_L}(Re_y, Tu, \lvert S \rvert)$
Turbulent energy production term	$P_{K_T} = P_{K_T}(Re_y, Tu, \lvert S \rvert)$
Energy transfer term	$R = R(Re_y, Tu, \lvert S \rvert)$

Simoni, Daniele et al. Modified formulation of Laminar Kinetic Energy transition models by means of elastic-net of a big experimental database of separated flows. Flow Turbulence and Combustion 105, 671–697 (2020)

Data reduction for transition modelling (LKE)

***Experimental and modelled** fragments of the **laminar energy production term** for the reference case: {Re=70000, Tu=1.5%, α=12deg}*

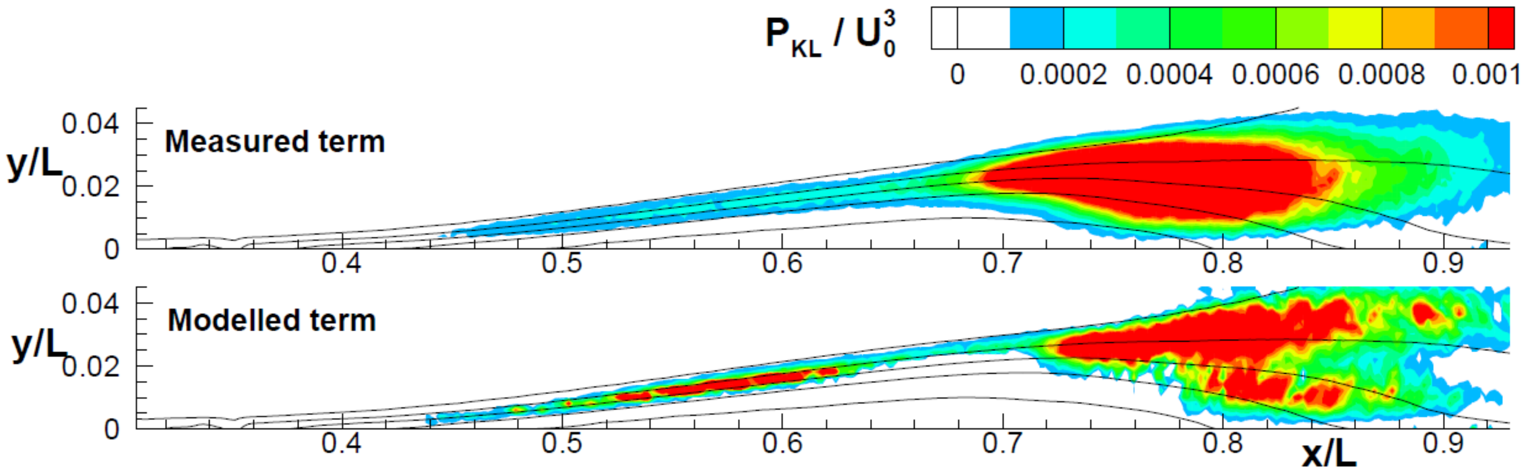

$$P_{K_L} = \overline{\widetilde{u_i}\widetilde{u_j}}\frac{\partial \overline{U}_i}{\partial x_j}$$

$$P_{K_L} = \frac{K_L^2}{\varepsilon}\left(\frac{\partial \overline{U}_i}{\partial x_j}\right)^2$$

- ***Same tendencies** between **the spatial distributions** of the two terms, high levels of P_{K_L} are detected within the separated shear layer and downstream of the bubble maximum displacement, where KH rolls develop*

Data reduction for transition modelling (LKE)

***Experimental and modelled** fragments of the **turbulent energy production term** for the reference case: {Re=70000, Tu=1.5%, α=12deg}*

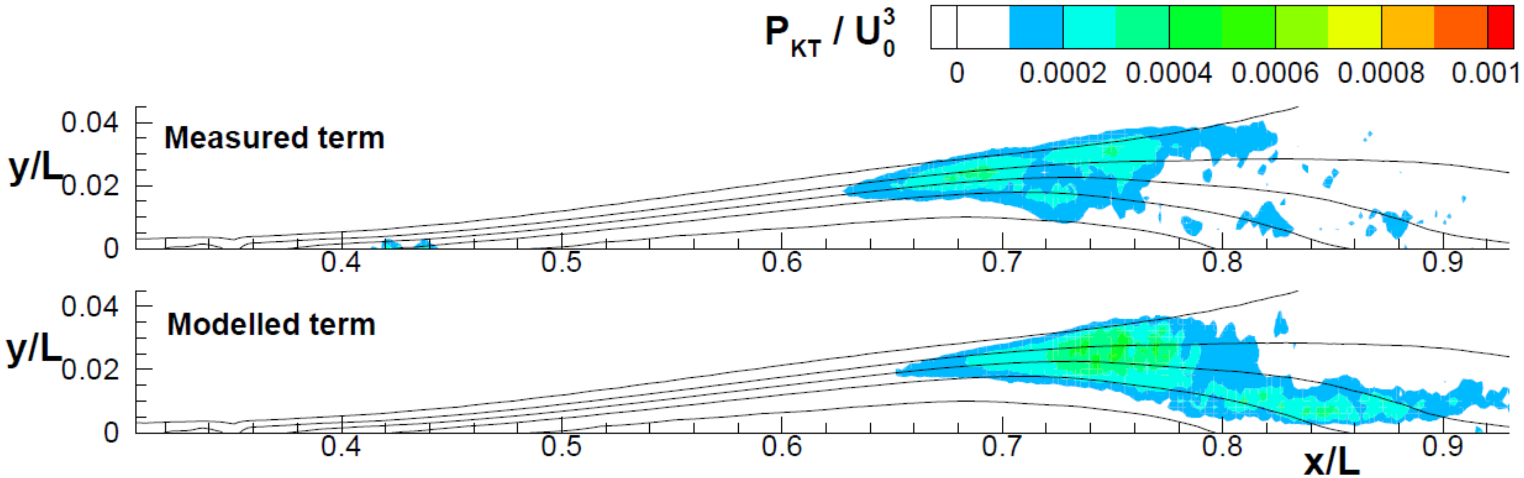

$$P_{K_T} = \overline{u_i' u_j'} \frac{\partial \overline{U}_i}{\partial x_j}$$

$$P_{K_T} = \frac{K_T^2}{\varepsilon} \left(\frac{\partial \overline{U}_i}{\partial x_j} \right)^2$$

- *Ability of the modeled term to reproduce the spatial distribution in the **bubble maximum displacement zone** and in the reattaching region where **KH rolls breackdown***

Data reduction for transition modelling (LKE)

Experimental and modelled *fragments of the* ***energy transfer term*** *for the reference case: {Re=70000, Tu=1.5%, α=12deg}*

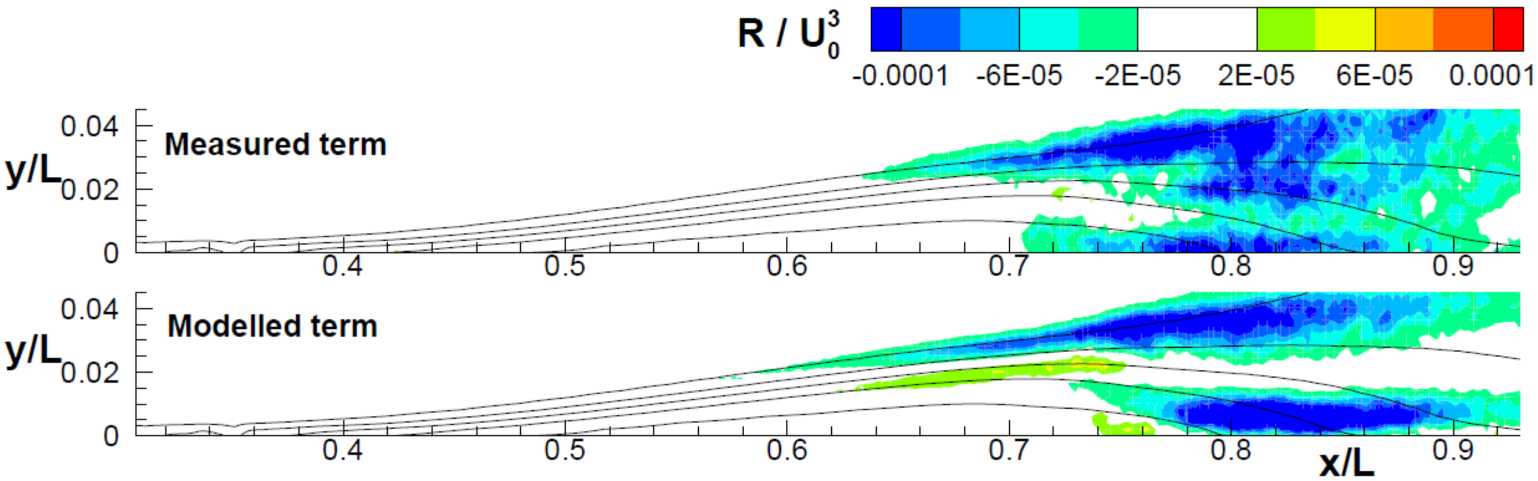

$$R = \overline{< u_i' u_j' > \frac{\partial \tilde{u}_i}{\partial x_j}}$$

$$R = \frac{K_T^2}{\mathbf{e}} \frac{\partial \overline{U}_i}{\partial x_j} \frac{\partial \tilde{u}_i}{\partial x_j}$$

- *Transfer term is* ***negligible in the separated shear layer*** *and becomes important around the bubble maximum displacement*
- *Good mimic between the measured and the modeled terms* ***downstream*** *the bubble maximum displacement*
  - ➢ ***Overall, the modeled term reproduces well the measured quantities***

Results and tuned models

- ***γ-Reθ*** *model*
- ***LKE*** *(Laminar Kinetic energy) model*
- ***Algebraic*** *models*

Algebraic transition models

- *Algebraic models are based on **non-linear** **algebraic** **constitutive laws** linking the stress tensor [τ] with the strain [S] and rotation [Ω] tensors,*
- *Algebraic models are able to consider also the **anisotropic** **character** of the turbulence, **overcoming** the limitations assumed in the Boussinesq's closure form.*

$$a_{ij} = \tau_{ij} - \frac{2}{3}k\delta_{ij} = \sum_n T_{ij}^{(n)} \nu_t^{(n)} = \nu_t'(I_1, I_2)T_{ij}^1 + \nu_t''(I_1, I_2)T_{ij}^2 + \nu_t'''(I_1, I_2)T_{ij}^3$$

- *For **2-D flows** the tensor basis is provided by **three elements** and related **apparent viscosities***

$$\begin{cases} T_{ij}^1 = S_{ij}^* \\ T_{ij}^2 = S_{ik}^*\Omega_{kj}^* - \Omega_{ik}^* S_{kj}^* \\ T_{ij}^3 = S_{ik}^* S_{ki}^* - \frac{1}{3}\delta_{ij} S_{mn}^* S_{mn}^* \\ I_1 = S_{mn}^* S_{mn}^* \\ I_2 = \Omega_{mn}^*\Omega_{mn}^* \end{cases}$$

$$\begin{cases} S_{ij}^* = \frac{1}{2\omega}\left(\frac{\partial U_i}{\partial x_j} + \frac{\partial U_j}{\partial x_i}\right) \\ \Omega_{ij}^* = \frac{1}{2\omega}\left(\frac{\partial U_i}{\partial x_j} - \frac{\partial U_j}{\partial x_i}\right) \end{cases}$$

*Here the **objective** is the **tuning** of the **apparent viscosities** also including different **flow features***

Algebraic transition models

- ***Two** independent **models** have been tuned**,** one **for short** and one **for long bubbles** type*

Bubble Classification:

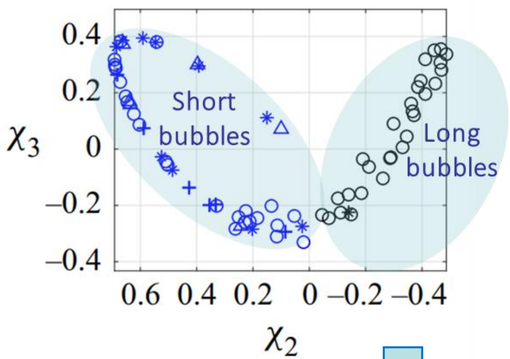

$$a_{ij}^{AG}(x) = w_{LB}(x)a_{ij}^{LB}(x) + w_{SB}(x)a_{ij}^{SB}(x)$$

Long separation bubble

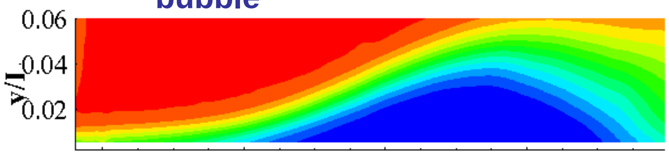

Short separation bubble

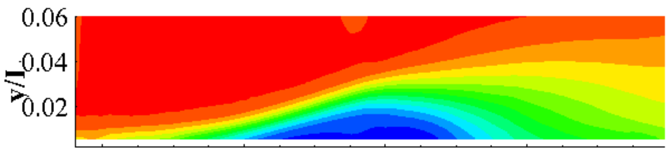

*Tune a **merged model that weights short and long cases** able to generally describe the Reynolds stress tensor for separated flow cases*

Dellacasagrande, M., et al. "A data-driven analysis of short and long laminar separation bubbles." *Journal of Fluid Mechanics* 976 (2023)

Algebraic transition models: promoting sparsity

Different models tuned with SBL** are evaluated on a **Validation Set** varying the **sparsity promoting term λ:

- ***Increasing λ, more sparse** models are obtained*
- *A **trade-off** between **accuracy/generalizability** is searched*

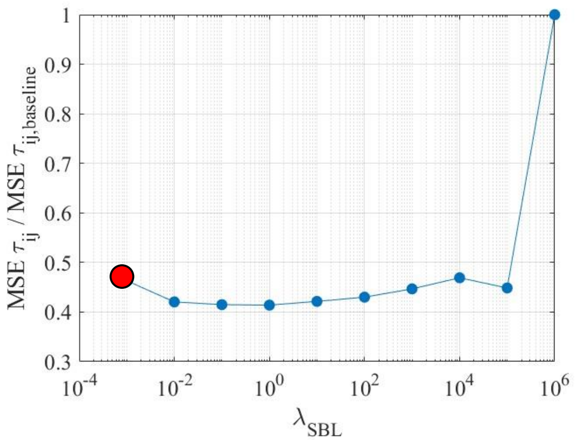

Measured Components

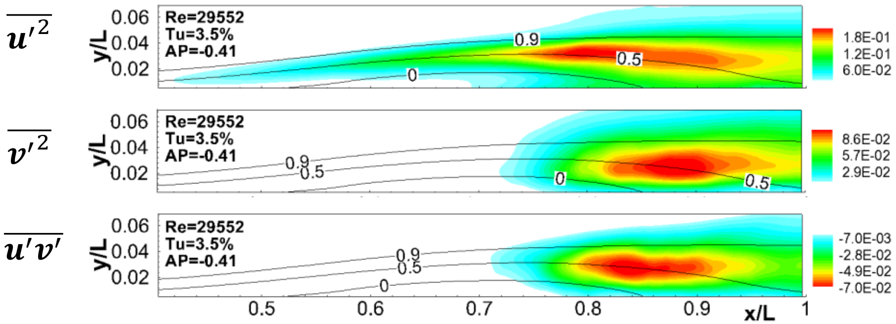

Modelled Components $\lambda = 10^{-3}$

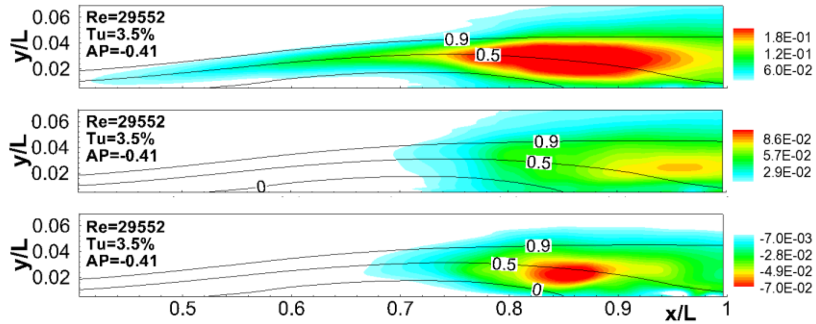

Carlucci A. et al. An Experimental Database for Machine Learning of Algebraic Models in Separated Flows, under review in FTC, 2024

Algebraic transition models: promoting sparsity

Different models tuned with SBL *are evaluated on a* ***Validation Set*** *varying the* ***sparsity promoting term λ:***

- ***Increasing λ, more sparse*** *models are obtained*
- *A* ***trade-off*** *between* ***accuracy/generalizability*** *is searched*

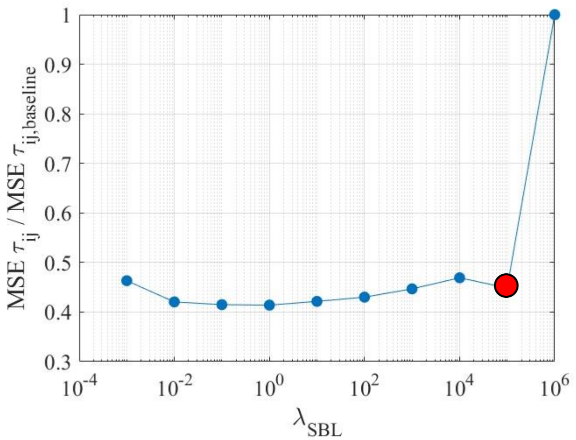

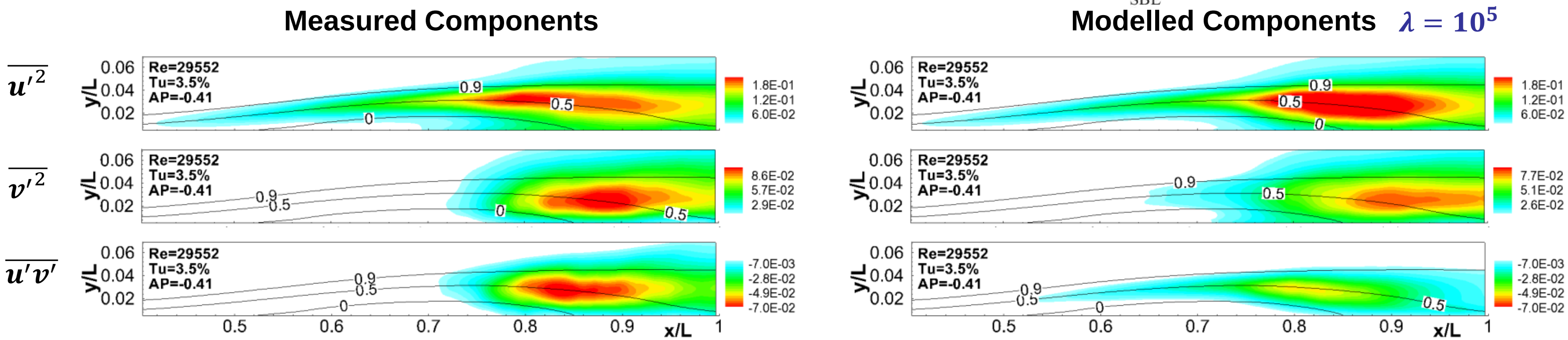

Carlucci A. et al. An Experimental Database for Machine Learning of Algebraic Models in Separated Flows, under review in FTC, 2024

Algebraic transition models: promoting sparsity

Different models tuned with SBL *are evaluated on a* ***Validation Set*** *varying the* ***sparsity promoting term λ:***

- ***Increasing λ, more sparse*** *models are obtained*
- *A* ***trade-off*** *between* ***accuracy/generalizability*** *is searched*

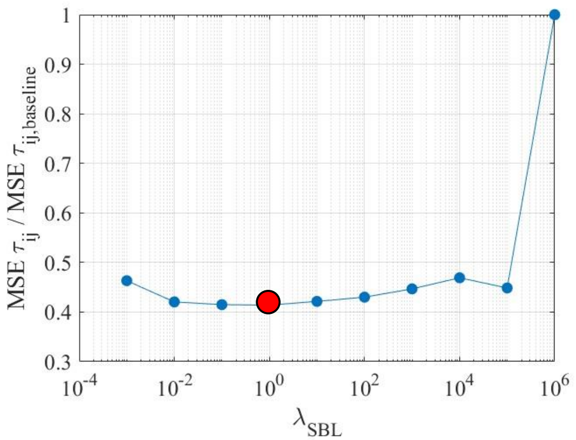

Measured Components **Modelled Components** $\lambda = 1$

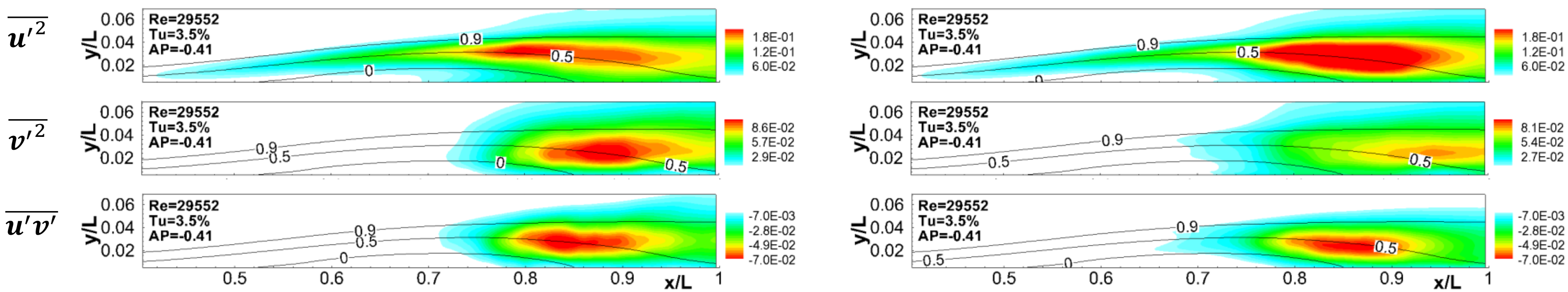

Carlucci A. et al. An Experimental Database for Machine Learning of Algebraic Models in Separated Flows, under review in FTC, 2024

Algebraic transition models: promoting sparsity

Different models tuned with SBL** are evaluated on a **Validation Set** varying the **sparsity promoting term λ:

- ***Increasing λ, more sparse** models are obtained*
- *A **trade-off** between **accuracy/generalizability** is searched*

Predictor	Tensor	Coefficient	Uncertainty
cost.	T_{ij}^1	-0.068	1.0%
cost.	T_{ij}^2	-1.1	0.092%
$I_{2\Omega}$	T_{ij}^1	-0.42	0.38%
I_{2S^2}	T_{ij}^1	-0.1	15%
$I_{2S}^5 I_{2\Omega}^5$	T_{ij}^1	-55	0.51%
$I_{2\Omega}$	T_{ij}^2	-0.32	0.056%
I_{2S}^5	T_{ij}^2	2.2	0.31%
$I_{2S}^5 I_{2\Omega}^5$	T_{ij}^2	21	0.93%
$I_{2\Omega}$	T_{ij}^3	1.8	0.46%
$I_{2\Omega}^2$	T_{ij}^3	5.1	0.34%

Measured Components

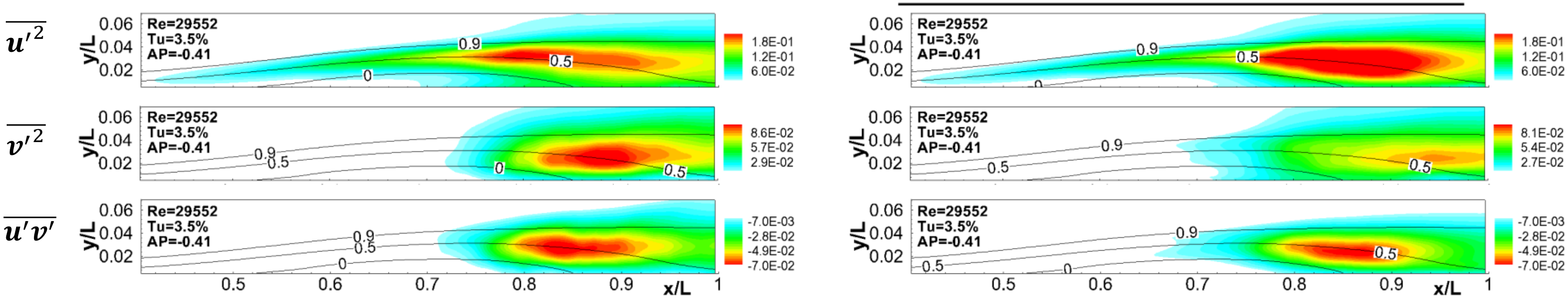

Carlucci A. et al. An Experimental Database for Machine Learning of Algebraic Models in Separated Flows, under review in FTC, 2024

Algebraic transition models: weight between models

*The **final model** will be obtained **combining both short and long bubbles** model*

*The **weighting terms** have been **tuned,** with possible choice of the **hyperparameter σ_w***

$$w_{SB}(x,\sigma_w) = \frac{g_{SB}(x,\sigma_w)}{g_{SB}(x,\sigma_w) + g_{LB}(x,\sigma_w)}$$

$$a_{ij}^{AG}(x) = w_{LB}(x)a_{ij}^{LB}(x) + w_{SB}(x)a_{ij}^{SB}(x)$$

$$g_{SB,LB} = \exp\left(-\frac{1}{2}\frac{\sum_{i=1}^{2}\sum_{i=j}^{2}(p_{ij}(a_{ij}^{SB,LB}-a_{ij})^2)}{\sigma_w^2}\right)$$

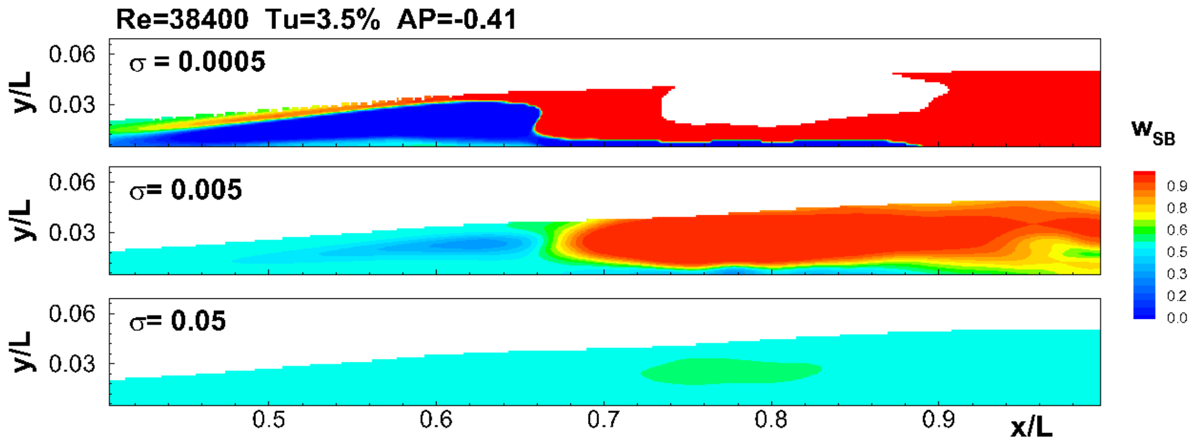

Algebraic transition models: merging the models

*Once the **"specialized" models** for **short and long bubbles** are tuned, **an aggregated model (AG)** can be obtained and tested on intermediate flow cases*

$$\boldsymbol{\tau}_{\boldsymbol{ij}}^{\Delta(\boldsymbol{AG})} = w_1 \boldsymbol{\tau}_{\boldsymbol{ij}}^{\Delta(\boldsymbol{short})} + w_2 \boldsymbol{\tau}_{\boldsymbol{ij}}^{\Delta(\boldsymbol{long})} \qquad \begin{cases} \sum_i w_i = 1 \\ w = w(flow\ features, \dots) \end{cases}$$

Measured Components

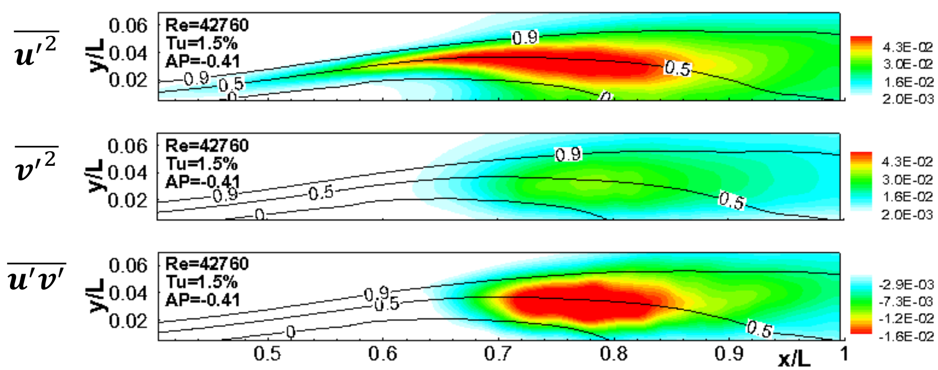

Modelled Components

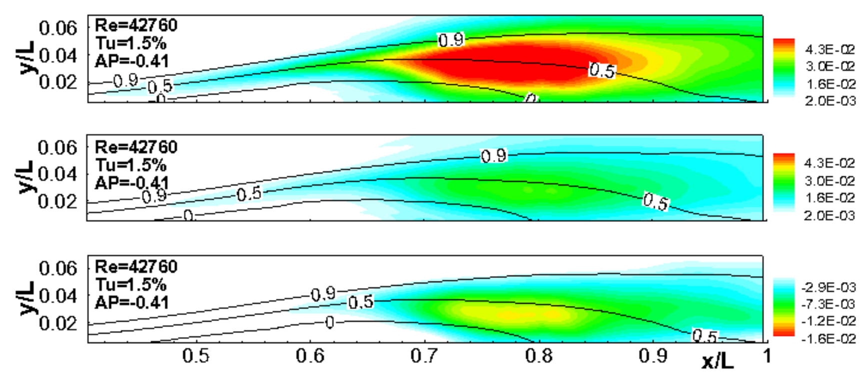

Algebraic transition models: merging the models

*Adding **flow features** increases significantly the **prediction accuracy***

feature	definition
η_1	$\frac{\lVert\Omega\rVert^2-\lVert S\rVert^2}{\lVert\Omega\rVert^2+\lVert S\rVert^2}$
η_2	$\frac{k}{0.5U_iU_i+k}$
Re_k	$\frac{\sqrt{k}y}{\nu} * 10^{-2}$
Re_{k_x}	$\frac{\sqrt{k}x}{\nu} * 10^{-3}$
Re_Ω	$\frac{\sqrt{I_2}y^2}{\nu} * 10^{-1}$
Re_{Ω_x}	$\frac{\sqrt{I_2}x^2}{\nu} * 10^{-3}$
Π_2	$\frac{\lVert\Omega\rVert y}{\lVert U\rVert} * 10^{-1}$
Π_5	$\frac{k}{\nu\lVert\Omega\rVert} * 10^{-2}$
Π_6	$\frac{\lVert S\rVert y}{\lVert U\rVert} * 10^{-2}$
Π_k	$\frac{\lVert S\rVert y}{\sqrt{k}} * 10^{-1}$

$$\boldsymbol{\tau}_{\boldsymbol{ij}}^{\Delta(\boldsymbol{AG})} = w_1\boldsymbol{\tau}_{\boldsymbol{ij}}^{\Delta(\boldsymbol{short})} + w_2\boldsymbol{\tau}_{\boldsymbol{ij}}^{\Delta(\boldsymbol{long})}$$

$$\begin{cases} \sum_i w_i = 1 \\ w = w(flow\ features, \dots) \\ \nu_t^{',\dots,'''}(I_1, I_2, flow\ features, \dots) \end{cases}$$

Measured Components

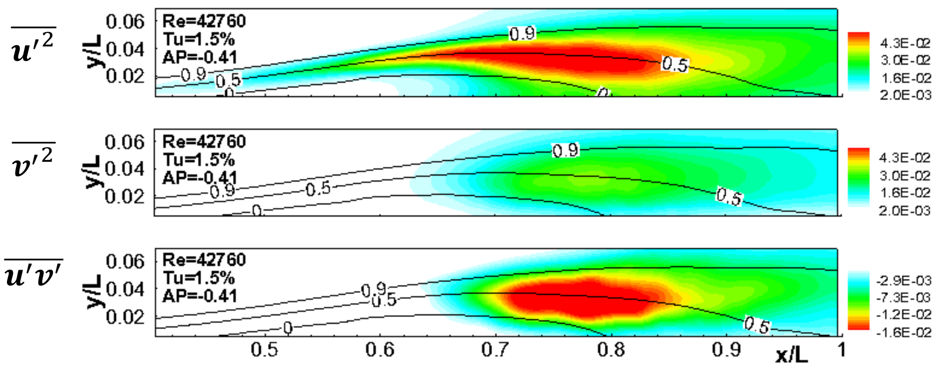

Modelled Components

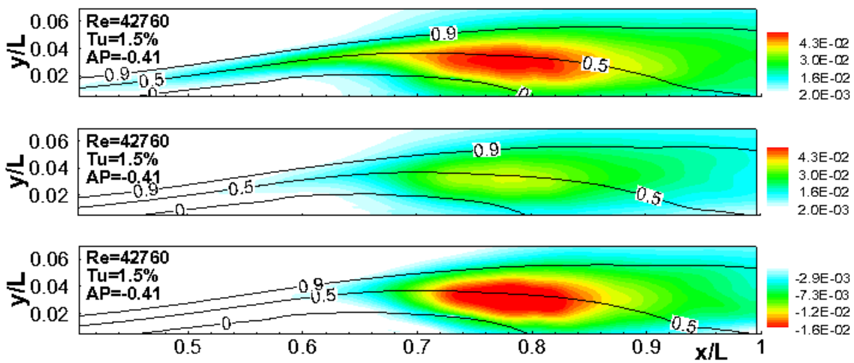

Thank you for your attention

Principal axes analysis

Separated flow transition case

Strain tensor

Deviatoric part of the stress tensor

***Principal directions**:*

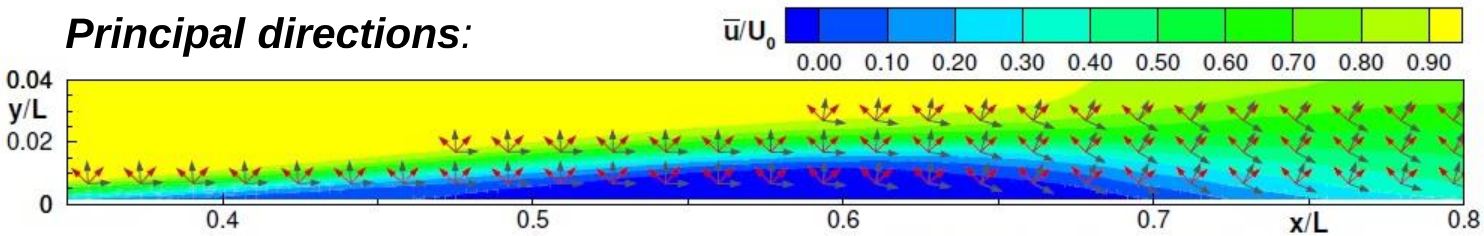

- *The **shear orientation** is **±45°** with respect to the wall normal direction.*

***Magnitudes**:*

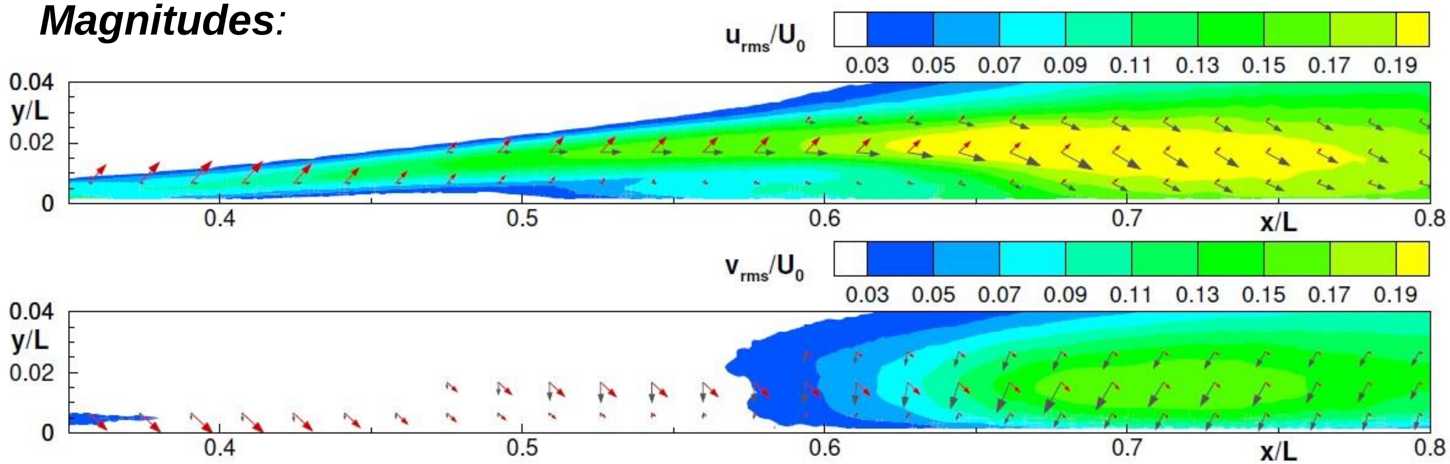

- *The **stress principal directions** start to **incline** in correspondence of the bubble maximum displacement.*

Principal axes analysis

By-pass flow transition case

→ ***Shear stress tensor***

→ ***Deviatoric part of the stress tensor***

Principal directions:

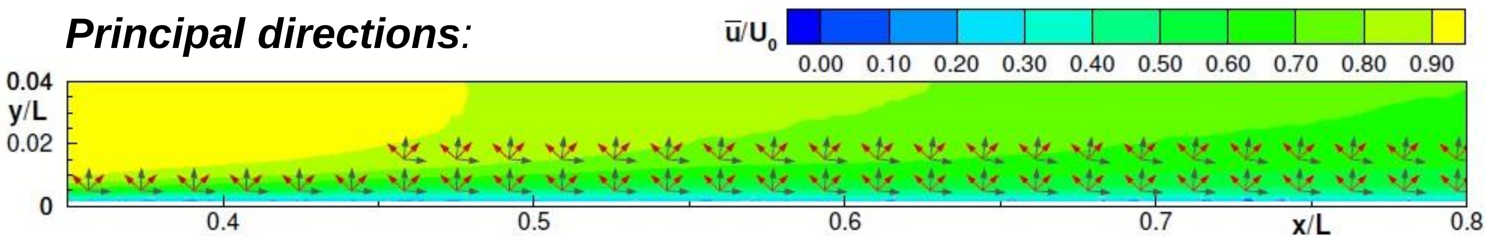

- *The **shear orientation** is $\pm$**45°** with respect to the wall normal direction.*

Magnitudes:

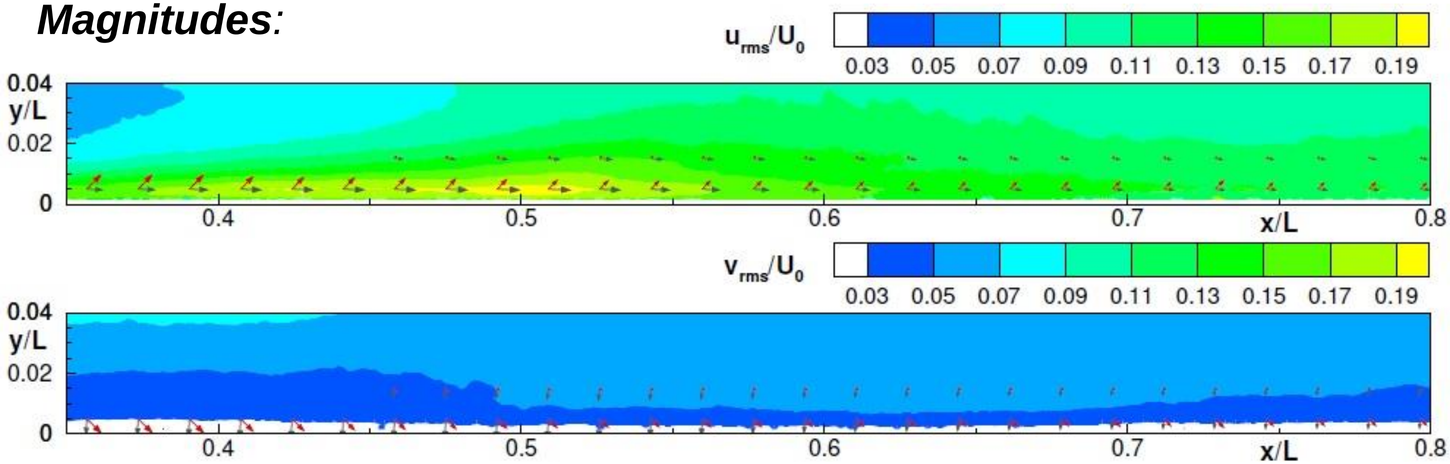

- *The **stress principal directions** remain aligned with the streamwise direction. The dominant term driving the by-pass transition is $\overline{u'^2}$ and the process is characterized by a **strong anisotropy**.*

Algebraic transition models

- *For example, the Pope's tensorial expansion provides the constitutive law:*

$$[\tau] = \nu_T[S] + \nu'_T[S][\Omega] + \nu''_T[S][S]^T + \nu''_T[S][\Omega][S]^T + \cdots$$

*where practically the sum of **higher order** tensor elements **modifies the principal axes** (both **rotating** and **stretching**) of the modelled turbulent stress tensor.*

- *A variant of classic algebraic relations **has been proposed**, involving:*
  - *A **rotation matrix** $[R]$ providing a **local re-orientation** of the principal axes*
  - *A **diagonal matrix** $[\Delta_\nu]$ providing the **local stretching** of the principal axes*

$$[\tau] = [X_s][R][\Delta_\nu][\Delta_s][R]^T[X_s]^T$$

where:

$$[R] = \begin{bmatrix} \cos\theta & \sin\theta \\ -\sin\theta & \cos\theta \end{bmatrix}$$

$[\Delta_S]$ *diagonal matrix of the eigenvalues of the strain tensor*

$$[\Delta_\nu] = \begin{bmatrix} \nu_I & 0 \\ 0 & \nu_{II} \end{bmatrix}$$

$[X_S]$ *matrix of the eigenvectors of the strain tensor*

Lengani, Davide et al. Analysis and Modeling of the Relation Between Shear Rate and Reynolds Stress Tensors in Boundary Layer Transition, Submitted to HFF.

Data reduction

- *A **polynomial fitting strategy** is used to define a relationship f and f' for the **stress eigenvalue** $\lambda_{1,\tau}$ and for the **displacement angle** $\Delta\theta$ in function of known flow properties: the **turbulent kinetic energy** k, the ℓ2 **norm of the shear tensor** $|S|$ and the **Reynolds number** Re_y.*

$$\lambda_{1,\tau} = f(k, |S|, Re_y)$$
$$\Delta\theta = f'(k, |S|, Re_y)$$

where Re_y is based on the wall distance y and the local velocity outside the BL u_{ext}.

- *The **relationship** for $\lambda_{1,\tau}$ and $\Delta\theta$ can be included to **model the stress tensor** by means of the previous definition:*

$$[\tau_{mod}] = [X_s][R]\left[\Delta_{\tau,mod}\right][R]^T[X_s]^T$$

with:

$$[R] = \begin{bmatrix} \cos\Delta\theta_{mod} & \sin\Delta\theta_{mod} \\ -\sin\Delta\theta_{mod} & \cos\Delta\theta_{mod} \end{bmatrix} \qquad [\Delta_{\tau,mod}] = \begin{bmatrix} \lambda_{1,\tau} & 0 \\ 0 & -\lambda_{1,\tau} \end{bmatrix}$$

Data reduction

Model validation

- *The model capability was tested **comparing** the **modeled results** with the **experimental measurements** for two different flow conditions that did not participate to the education of the model.*

Separated flow transition

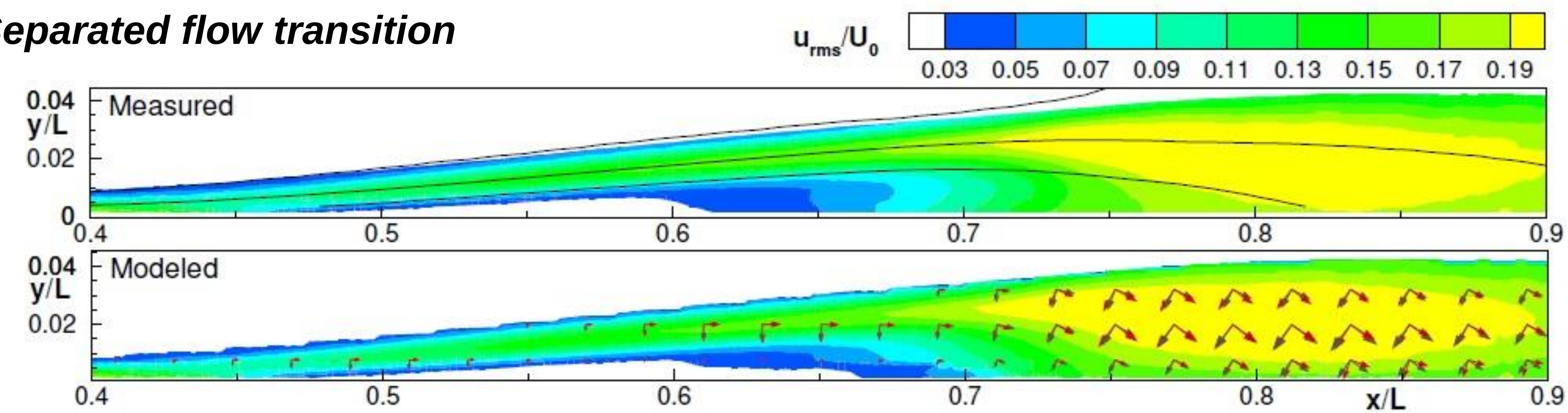

***Measured eigenvectors** of the **stress** tensor*

***Modeled eigenvectors** of the **stress** tensor*

Data reduction

Model validation

- *The model capability was tested **comparing** the **modeled results** with the **experimental measurements** for two different flow conditions that did not participate to the education of the model.*

By-pass flow transition

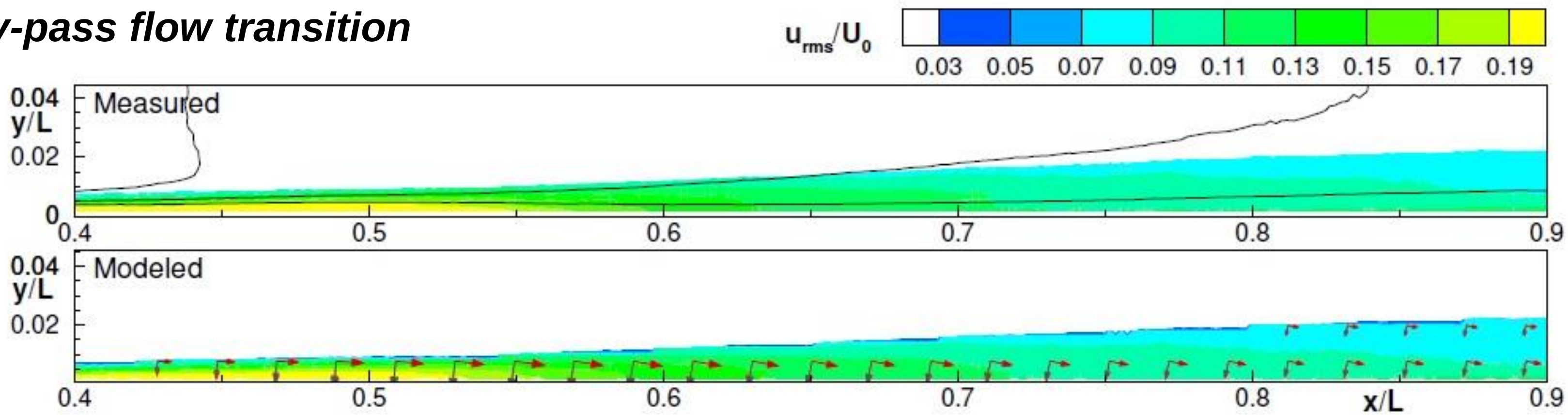

Measured eigenvectors *of the* ***stress*** *tensor*

Modeled eigenvectors *of the* ***stress*** *tensor*

- *The distributions are **well reproduced**, always capturing the **correct orientation and magnitude** of the **stress eigenvectors**. Some small discrepancy are showed just in the end region close to the wall.*

Learning Procedure for tuning

Details about the application of the Elastic Net

The data are organized in:

- $[\boldsymbol{Y}]_{NX1}$ *is the targeting function (N observations)*
- $[\boldsymbol{X}]_{NXM}$ *is the Vandermonde matrix (N observations, M predictor functions)*

The ***targeting function*** *is :* $\widehat{\boldsymbol{\beta}} = arg_{\beta}\min[|\boldsymbol{Y} - \boldsymbol{X}\,\boldsymbol{\beta}|^2 + \lambda_1|\boldsymbol{\beta}| + \lambda_2|\boldsymbol{\beta}|^2]$

To find the model coefficients $\widehat{\beta}$ *the argument of the targeting function is derived for the case* $\lambda_2 \neq 0$ *and* $\lambda_1 = 0$*, obtaining:*

$$\widehat{\boldsymbol{\beta}}_{en} = \left(\frac{\boldsymbol{X}^T\boldsymbol{X} + \lambda_2\boldsymbol{I}}{1+\lambda_2}\right)^{-1}\boldsymbol{X}^T\boldsymbol{Y}$$

The ℓ_1 *norm is then applied solving the equation for* $\widehat{\boldsymbol{\beta}}_{en}$ ***iterratively*** *and setting a* ***threshold*** λ_1 *to actuate the* ***variable selection****.*

Learning Procedure for tuning

Details about the application of the Elastic Net

*A **mask matrix $\boldsymbol{M}$** consisting of 1 and 0 elements is defined to identify the **surviving predictors***

The reduced model $\boldsymbol{Y}_{en}$ can be estimated as: $\boldsymbol{Y}_{en} = \boldsymbol{X}\boldsymbol{M}\widehat{\boldsymbol{\beta}}_{\boldsymbol{en}}$

*The **best combination** of the penalization coefficients (λ_1,λ_2) is identified throught the inspection of the **residual** and of the **overall number** of model coefficients:*

$$R = ||\boldsymbol{Y}_{en} - \boldsymbol{X}\boldsymbol{M}\widehat{\boldsymbol{\beta}}_{\boldsymbol{en}}||^{\boldsymbol{2}}$$

Principal axes analysis

- *A **principal axis analysis** has been performed on the available **experimental data set**.*

*For consistency (respect of the tensor properties), the **deviatoric part of the Reynolds stress tensor** [$\hat{\tau}$] and the **shear rate tensor** [$\hat{S}$] were analyzed.*

$$[\hat{\tau}] = \begin{bmatrix} \frac{1}{2}\left(\overline{u'u'} - \overline{v'v'}\right) & \overline{u'v'} \\ \overline{u'v'} & \frac{1}{2}\left(\overline{v'v'} - \overline{u'u'}\right) \end{bmatrix}$$

$$[\hat{S}] = \begin{bmatrix} \frac{1}{2}\left(\frac{\partial \overline{U}}{\partial x} - \frac{\partial \overline{V}}{\partial y}\right) & \frac{1}{2}\left(\frac{\partial \overline{U}}{\partial y} + \frac{\partial \overline{V}}{\partial x}\right) \\ \frac{1}{2}\left(\frac{\partial \overline{U}}{\partial y} + \frac{\partial \overline{V}}{\partial x}\right) & \frac{1}{2}\left(\frac{\partial \overline{V}}{\partial y} - \frac{\partial \overline{U}}{\partial x}\right) \end{bmatrix}$$

*In this way, the tensors have the same structure (trace null and symmetric) and **eigenvalues and eigenvectors** can be **compared,** being both of the form:*

$$[\Delta] = \begin{bmatrix} \lambda_1 & 0 \\ 0 & -\lambda_1 \end{bmatrix} = \begin{bmatrix} \sqrt{A^2 + C^2} & 0 \\ 0 & -\sqrt{A^2 + C^2} \end{bmatrix}$$

$$[X] = \begin{bmatrix} \lambda_1 + A + C & -\lambda_1 - A + C \\ \lambda_1 + A - C & -\lambda_1 + A + C \end{bmatrix}$$

where: A the off-diagonal elements

C the positive diagonal term

Data reduction

- ***The*** ***eigenvalue*** $\lambda_{1,\tau}$ *of the* ***deviatoric stress tensor*** *normalized with the turbulent kinetic energy has been computed.*

- ***The*** ***displacement angle*** $\Delta\theta$ ***between*** *the first eigenvector of the* ***shear*** *and the first of the* ***stress*** *tensor was also calculated.*

Separated flow transition case

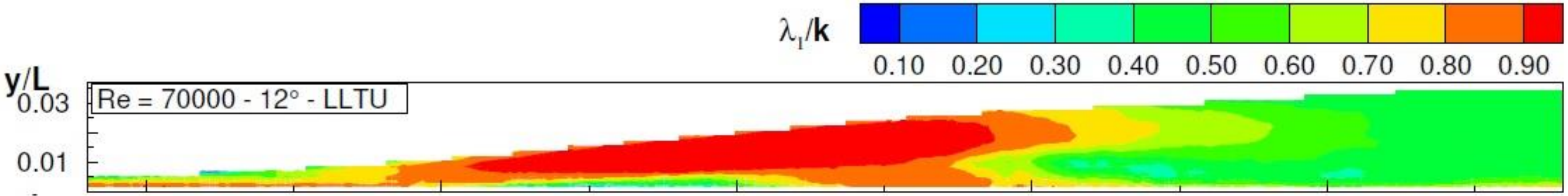

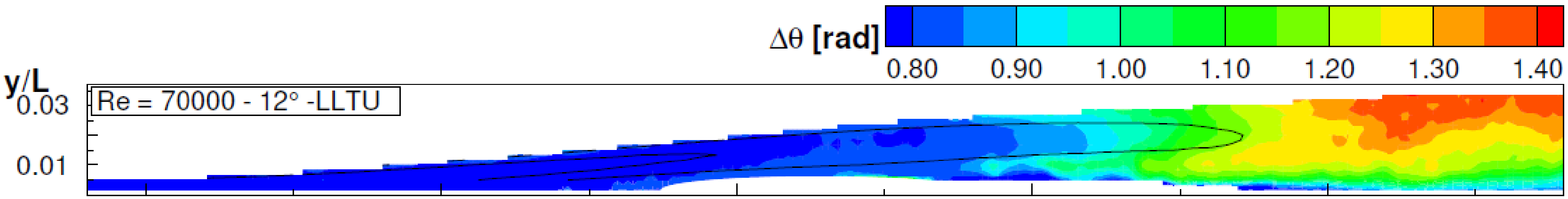

Data reduction for transition modelling (Algebraic)

- ***The*** ***eigenvalue*** $\lambda_{1,\tau}$ *of the* ***deviatoric stress tensor*** *normalized with the turbulent kinetic energy has been computed.*

- ***The*** ***displacement angle*** $\Delta\theta$ ***between*** *the first eigenvector of the* ***shear*** *and the first of the* ***stress*** *tensor was also calculated.*

By-pass flow transition case

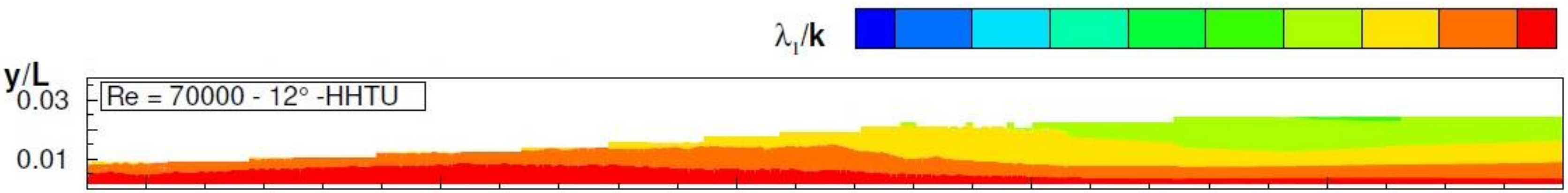

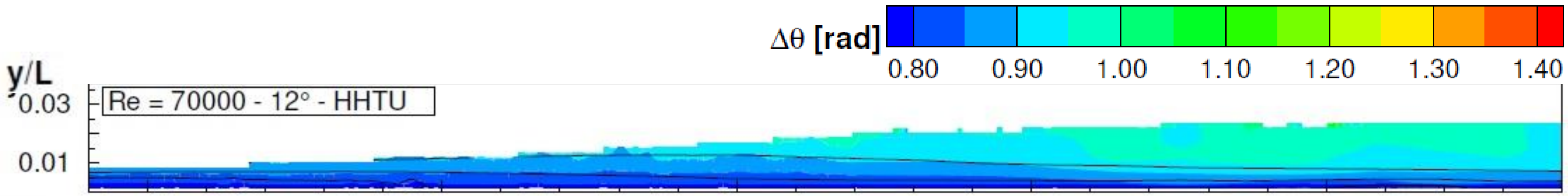

Experimental setup

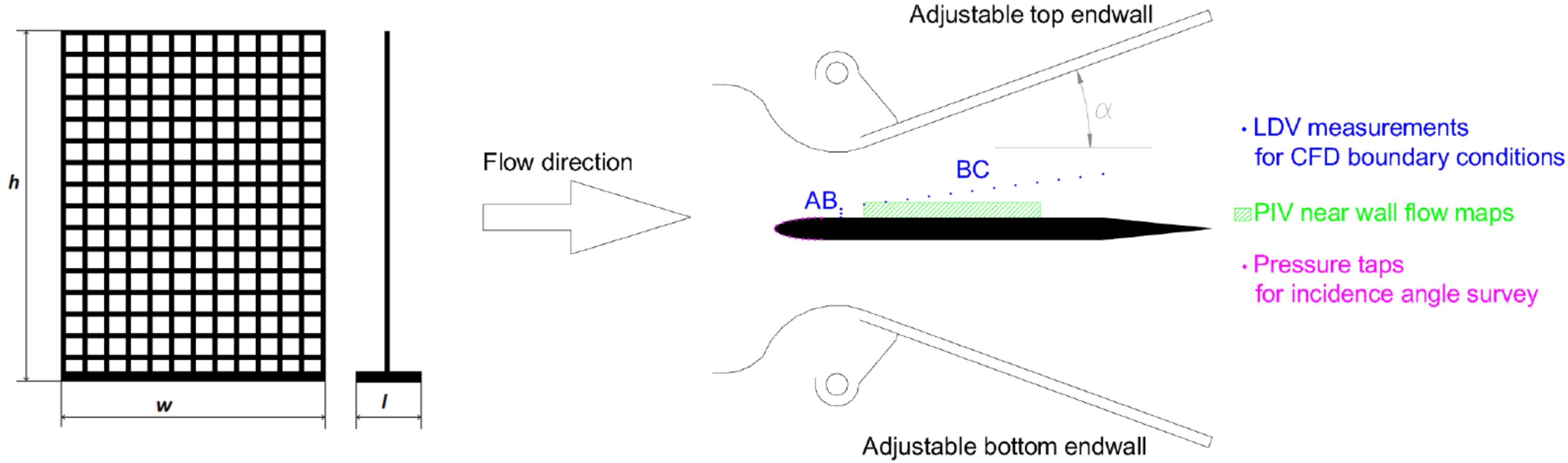

- ***Flat plate*** *installed within adjustable endwalls to control the pressure gradient. Upstream, different turbulence generating grids are adopted to test different free-stream turbulence intensity.*

  - *Boundary layer transition is experimentally characterized for variable* ***Reynolds numbers, free-stream turbulence intensities*** *and* ***adverse pressure gradients****.*

Measuring techniques

Fast-Response Particle Image Velocimetry & Laser Doppler Velocimetry

LASER SYSTEM:

- Double cavity Nd:Yag pulsed laser BLUESKY-QUANTEL CFR200
- Energy 2x100 mJ per pulse at 532 nm

CAMERA:

- Dantec High Sense digital camera
- 1280x1024 pixels cooled CCD matrix
- pixel dimension 6.7 μm
- 12 bit quantization
- Maximum frame rate in double frame mode: **3 kHz**

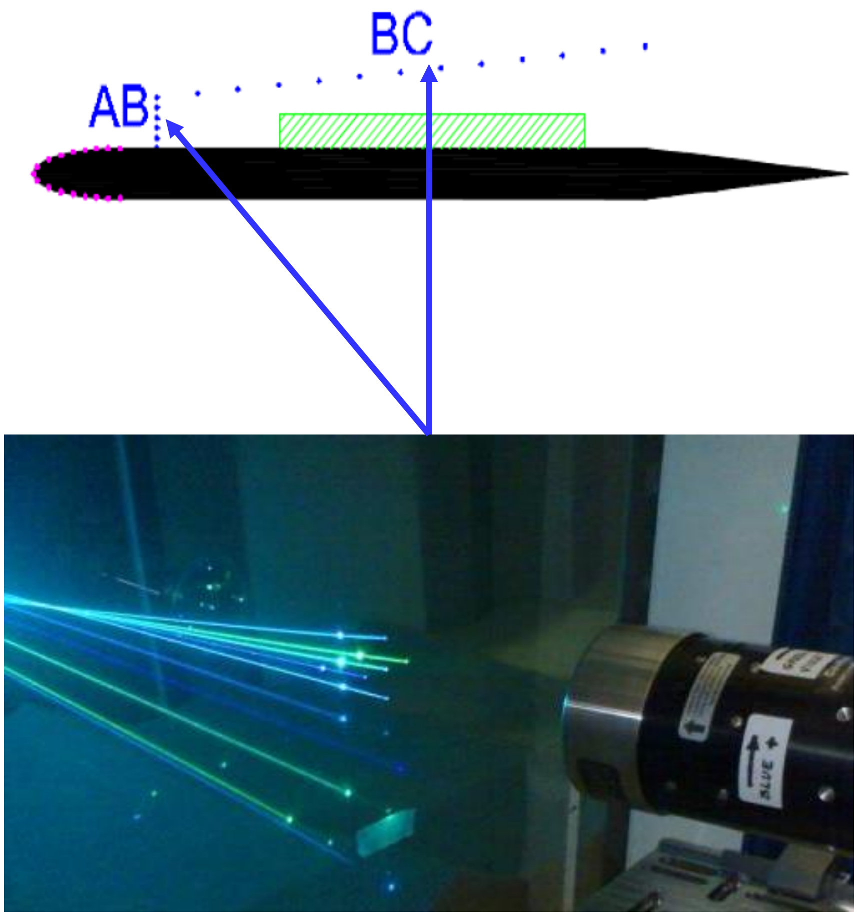

DANTEC FlowLite 2D LDV

- 200 mW 532 nm and 200 mW 488 nm solid state lasers
- Optical probe characteristics:

•Diameter	D=60 mm
•Beam separation before expansion	d= 38 mm
•Focal length	f=300 mm
•Beam intersection angle	$\theta = 7.2°$
•Probe volume	0.09x0.09x1.4 mm

Accurate data base on transitional flows

- **LDV boundary conditions for tuning of transition models**
  - **AB** line

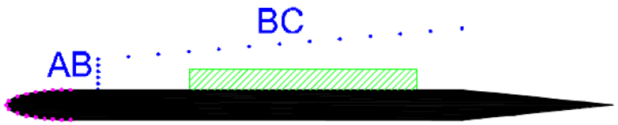

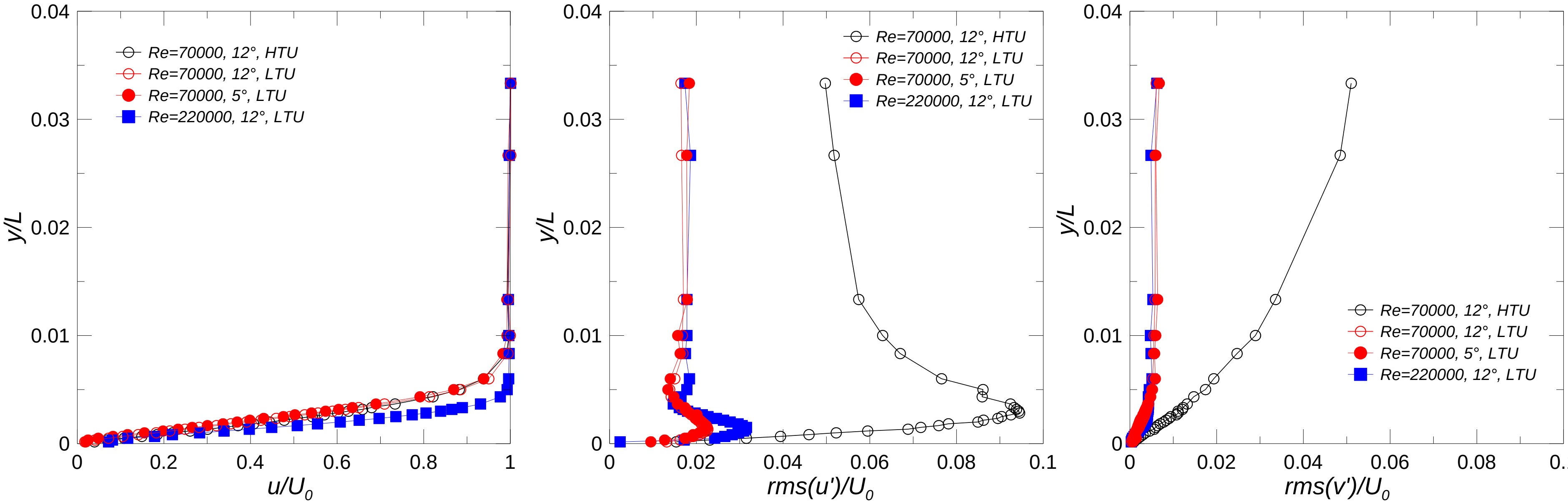

- Laminar velocity profiles: Re is the only parameter affecting the velocity profile;

- BL amplifies streamwise fluctuations whereas normal to the wall fluctuations are dumped.
  - Ordered streaks in pre-transitional BL are responsible of non-null streamwise fluctuations;